scientific reports



OPEN

Population genetic structure and demographic history of Dermacentor marginatus Sulzer, 1776 in Anatolia

Ömer Orkun^{©1⊠}, Eneshan Sarıkaya², Anıl Yılmaz², Mesut Yiğit³ & Zati Vatansever³

Dermacentor marginatus is a medically important tick species due to its preference humans and domestic animals as hosts and its vectorial competence, yet it remains understudied in many regions. This study aimed to examine the population structure and demographic history of D. marginatus using the cox1 and ITS2 genes, focusing on populations from Central and Northeast Anatolia—two regions on either side of the Anatolian Diagonal, a natural biogeographical barrier. A total of 361 host-seeking adult D. marginatus ticks from 31 sampling sites were analyzed, revealing 131 haplotypes for cox1 and 104 genotypes for ITS2. Neutrality tests and mismatch distribution patterns rejected the null hypothesis of the neutral theory, indicating that the population of D. marginatus in Anatolia has undergone a recent demographic expansion. Significant genetic differentiation and population structuring were observed between the Central and Northeastern Anatolian populations of D. marginatus, correlating with geographic distance and suggesting that the Anatolian Diagonal acts as a potential barrier to gene flow. Intrapopulation gene flow was higher in Central Anatolian populations compared to Northeastern Anatolian populations. Bayesian phylogeny revealed a highly divergent D. marginatus haplotype within the Northeastern Anatolian population, clustering into a Central Asian clade. Additionally, phylogenetic trees of the subgenus Serdjukovia revealed taxonomic ambiguities, including the absence of a distinct clade for D. niveus and potential misidentifications of D. marginatus and D. raskemensis specimens. Furthermore, the monophyletic relationship between D. marginatus and D. raskemensis supports the likelihood of sympatric speciation. These findings enhance our understanding of the genetic structure, phylogeography, and evolutionary dynamics of D. marginatus while providing a framework for future research on tick populations.

Keywords Dermacentor marginatus complex, Serdjukovia, Phylogeography, Tick evolution, cox1, ITS2

Studies on the population genetic structure of ticks are crucial for understanding their current and historical evolutionary processes, including demographic history, dispersal patterns, host adaptation, vectorial competence, and even chemical resistance^{1–3}. These insights can help characterize tick populations within and across geographic regions, shedding light on the processes driving genetic differentiation. Such knowledge is vital for developing more effective integrated control strategies, as it bridges the gap between the basic biology of vectors and the study of tick-borne pathogens⁴. Despite their importance, population genetic studies on ticks remain limited, leaving many species, species complexes, and groups in need of taxonomic and evolutionary clarification^{1,5}.

The genus *Dermacentor*, which includes several important vector species, remains understudied, with relatively limited genetic data available^{6–8}. *Dermacentor* species are widely distributed, in America's, Asia, and Europe, posing significant threats to human and animal health. The genus *Dermacentor* comprises approximately 40 species that share similar morphological characteristics, life cycles, seasonal activity patterns, host preferences, and ecology. However, the morphological identification of closely related species is often challenging, leading to potential errors in earlier reports^{8–11}. This highlights the need for comprehensive studies investigating the population structure of *Dermacentor* species to improve our understanding of this genus.

¹Ticks and Tick-Borne Diseases Research Laboratory, Department of Parasitology, Faculty of Veterinary Medicine, Ankara University, 06070 Ankara, Turkey. ²Graduate School of Health Sciences, Ankara University, Ankara, Turkey. ³Department of Parasitology, Faculty of Veterinary Medicine, Kafkas University, Kars, Turkey. [™]email: omerorkun@yahoo.com.tr

While recent researches have examined the population genetics of *Dermacentor* species in North America, such as *Dermacentor variabilis* and *Dermacentor andersoni* ^{12–15}, studies outside of this region are scarce. Most available data focus on *Dermacentor reticulatus* populations in Europe, leaving significant knowledge gaps for other species and geographic areas^{6,7,16–18}.

Dermacentor marginatus, also known as the ornate sheep tick, is one of the most important vector species within the genus Dermacentor^{10,19}. Its geographical distribution spans a wide range, including northern Africa (Morocco, Algeria, Tunisia), southern Europe up to northern France, northern Syria, Türkiye, and extending from Iran and Russia to as far as China⁹. Ecologically, D. marginatus is well-adapted to warmer, drier climates in southern latitudes, thriving in steppes, alpine steppes, forest-steppes, and semi-desert areas^{19,20}. In Türkiye, it is reported across much of Anatolia, particularly in ecotones, such as transitional zones from forests to semi-arid areas, steppe landscapes, and, less frequently, forested habitats^{21–23}. Dermacentor marginatus serves as a competent vector for multiple pathogens, including the Crimean-Congo hemorrhagic fever virus, Omsk hemorrhagic fever virus, Spotted Fever Group rickettsiae, and Babesia caballi, playing a significant role in their ecology and epidemiology across various regions^{10,24,25}. Despite its importance as a vector and its broad distribution, the population genetic structure of D. marginatus remains largely unstudied in most of the areas where it occurs actively.

The subgenus Serdjukovia includes several closely related species, such as Dermacentor niveus, Dermacentor ushakovae, Dermacentor pomerantzevi, D. marginatus, Dermacentor raskemensis, Dermacentor silvarum, and Dermacentor nuttalli^{8,26}. However, this group still presents significant taxonomic challenges, with ongoing debates regarding the validity of some morphologically similar species, such as D. niveus and D. ushakovae. Past research has highlighted frequent misidentifications and inconsistencies in species classification, further complicating the taxonomy of this group^{8,9}. These uncertainties underscore the need for robust genetic characterization and population structure analyses to clarify the evolutionary relationships within the subgenus and resolve long-standing taxonomic ambiguities.

The Anatolian Diagonal, a prominent biogeographical feature of the Anatolian peninsula, has long been recognized as a natural barrier shaping the distribution and genetic divergence of numerous taxa. The Anatolian Diagonal is a natural biogeographical barrier that spans across Anatolia, influencing the distribution and genetic structure of many taxa. It consists of a series of mountain ranges and ecological transitions rather than a linear road or human-made structure. Studies on plant species, such as Turkish oaks (*Quercus* spp.), and vertebrates including the Anatolian ground squirrel (*Spermophilus xanthoprymnus*) and Levantine frog (*Hyla savignyi*) highlight the Diagonal's pivotal role in driving genetic differentiation and speciation^{27–31}. Similarly, arthropods like the meadow grasshopper (*Chorthippus parallelus*) and oak gall wasps (*Cynips quercus*) also exhibit genetic divergence across the Anatolian Diagonal, underscoring its broad influence on species distributions^{32–34}. Despite this well-documented impact on various taxa, the specific effects of the Anatolian Diagonal on the population genetics of tick species, such as *D. marginatus*, remain largely unexplored.

Phylogeographic studies are essential to understanding the detailed population genetic structure and phylogenetic relationships of *D. marginatus*. Therefore, this study aims to address this need by investigating the population genetic structure and demographic history of *D. marginatus* in Anatolia, focusing on populations located on both sides of the Anatolian Diagonal. By analyzing genetic data from tick samples collected in Central and Northeastern Anatolia, this research seeks to evaluate the role of the Anatolian Diagonal as a potential biogeographical barrier, influencing genetic differentiation and gene flow between populations. Furthermore, this research aims to explore whether the genetic patterns observed in *D. marginatus* populations correlate with those seen in other taxa influenced by the Diagonal, thus contributing to the broader understanding of its ecological and evolutionary impact.

The selection of these two study areas was primarily based on their significant geographical differences and their locations on either side (east and west) of the Anatolian Diagonal. We hypothesized that the distinct ecogeographical regions, combined with this barrier, might drive population structuring in *D. marginatus* populations across Anatolia. Additionally, *D. reticulatus*, another *Dermacentor* species, coexists with *D. marginatus* in mixed populations in both northern Central Anatolia and much of Northeastern Anatolia. The presence of *D. niveus*, a morphologically problematic species closely related to *D. marginatus*, has also been reported in these areas, especially in Northeast Anatolia^{35,36}. These factors could potentially increase genetic diversity or influence gene flow and restrictions between species, haplotypes, and genotypes in the same region.

Materials and methods Study area and sampling strategy

To ensure clarity and consistency throughout the study, we use specific terminology to describe different spatial scales. A pinpoint location refers to an exact geographical point where tick sampling was conducted. A sampling site encompasses multiple pinpoint locations within a defined ecological area and represents a broader collection zone. The study focuses on two major regional populations, Central Anatolia (CN) and Northeastern Anatolia (NE), which serve as the primary units for population genetic comparisons.

The study area was divided into two ecogeographical regions, located in Central and Northeastern Anatolia of Türkiye, which provide suitable habitats for *D. marginatus*. The CN is situated along a key ecotone, beginning with the forested phytogeography of the western Black Sea in the north, transitioning into the semi-arid Irano-Turanian steppe zone, and extending to the Kızılırmak River, continuing toward the Polatlı and Seyfe plains, which exhibit a varying steppe structure. The NE spans from the forested areas of the eastern Black Sea, through high Alpine-type grasslands and plateaus dominated by Irano-Turanian phytogeography, to the valley ecosystem of the Aras River, reaching the Armenian border (Fig. 1).

Sampling sites in both regions (CN and NE), were defined based on geographic, abiotic, and ecological factors, such as grazing distances for domestic ruminants and the displacement of wild boars. *Dermacentor*

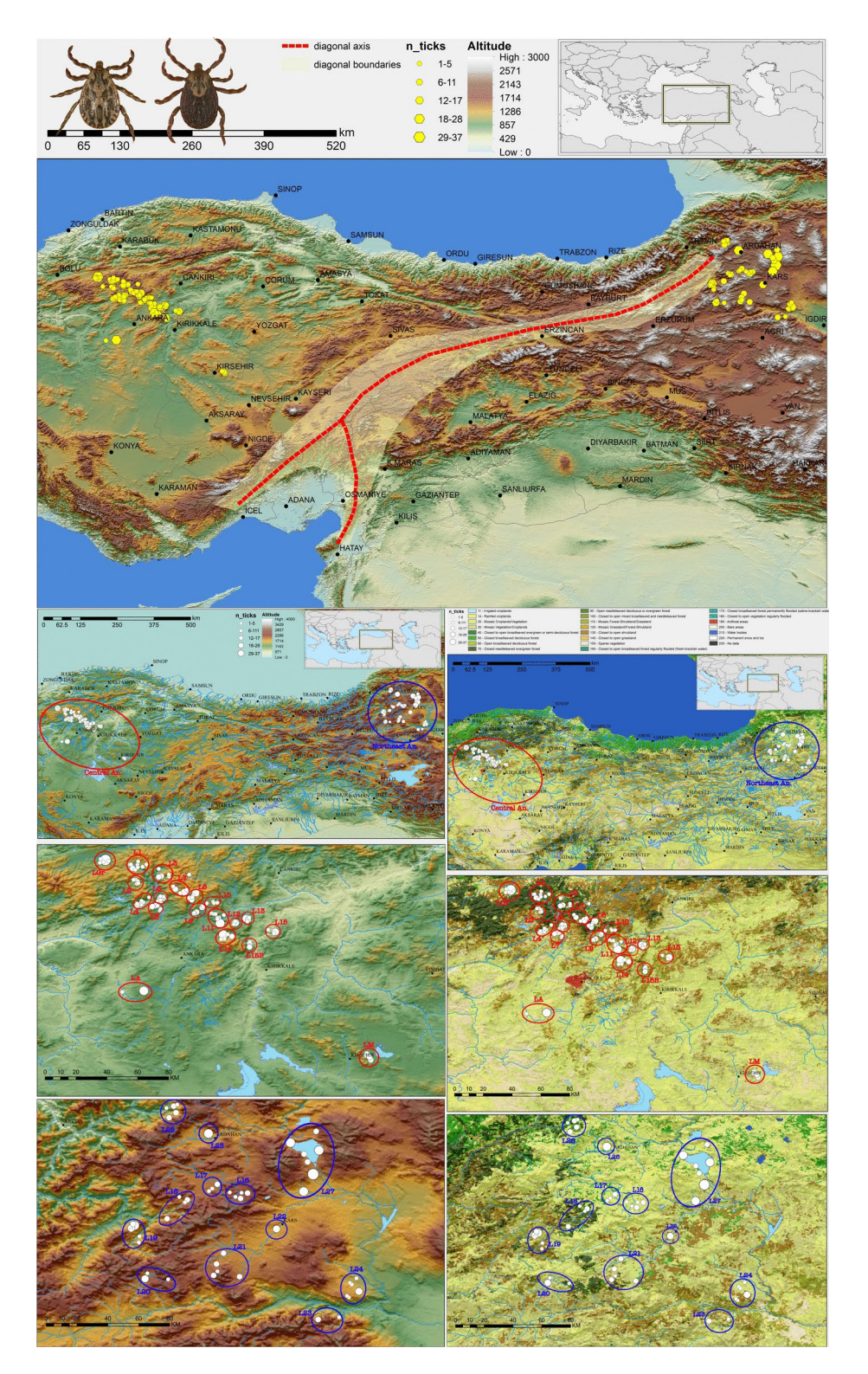


Fig. 1. Maps showing the study areas and locations where *Dermacentor marginatus* specimens were collected. Sampling sites determined in this study are indicated on both elevation and vegetation-based maps. The position of the Anatolian Diagonal on the map is drawn based on Kuzguncuoğlu et al. (2019). Maps were generated using ArcGIS 10.6.1 software, and the final figure composition was created using Inkscape 1.2.

marginatus has a three-host life cycle, with immatures displaying an endophilic (nidicolous) behavior, feeding primarily on small rodents without leaving their habitat. Adults, however, mostly prefer larger ungulates—such as ruminants, equids, and wild boars—as hosts¹⁰. Notably, migratory birds and frequently displaced native birds are not part of *D. marginatus*' natural host preference, limiting its mobility, which is primarily influenced by the

movement of large animals. This leads to the formation of more isolated populations in confined areas. A total of 31 sampling sites were identified, including 19 in CN and 12 in NE regions. The sampling sites were mapped using ArcGIS 10.6.1 (Esri, 2018) and geographic information systems (GIS) (Fig. 1). Detailed information on each sampling site, including name, center coordinates, district/province, altitude, land/vegetation structure, climate type, average annual temperature, average annual relative humidity, and total annual precipitation, is provided in Table S1. Climatic data were sourced from the nearest measurement stations of the General Directorate of Meteorology, using an average value from the last 30 years.

Performing power analyses in tick population genetics is challenging due to limited prior data on tick population densities. Consequently, such analyses are rarely applied in classical population genetics studies focusing on differentiation or gene flow. Instead, researchers prioritize broad geographic and ecological coverage to ensure robust sampling, as is common in many tick studies^{3,18}. In this study, we employed a comprehensive sampling strategy, selecting 361 host-seeking adult *D. marginatus* from 31 sampling sites across Anatolia. This approach aimed to capture genetic diversity within *D. marginatus* populations and ensure sufficient representation for detecting population structure and demographic patterns.

Tick collection and morphological identification

Host-seeking adults of *D. marginatus* were collected from 151 pinpoint locations across 31 sampling sites (Fig. 1). Tick collection took place over four seasons of *Dermacentor* activity: fall 2021, spring 2022, fall 2022, and spring 2023, spanning from September 2021 to August 2023. Ticks were collected during daylight hours using a 1.5×1 m white cotton cloth, which was dragged over vegetation, or by hand when visually encountered. The collected ticks were placed in air-permeable vials, labeled according to their location, and recorded with geographical information. Ticks from CN were transported to the Ticks and Tick-borne Diseases Research Laboratory (TTBDRL) at Ankara University's Faculty of Veterinary Medicine under suitable conditions on the same day. Ticks from NE were similarly transported to the Department of Parasitology at Kafkas University on the same day, and subsequently, specimens were transported alive to TTBDRL within a week.

The morphological identification of tick specimens was performed using a stereo microscope (Stemi 2000-C, Zeiss, Germany) equipped with and AxioCam digital camera and ZEN software, following standard taxonomic keys^{26,37-40}. After morphological identification, each tick was washed in 70% ethanol, rinsed in sterile DNase/RNase-free water, and dried on sterile filter paper. The specimens were then placed in sterile tube and stored at -80 °C until further molecular analysis.

Nucleic acid extraction, PCR, and sequencing

Tick samples included in the molecular analysis, were individually homogenized in bead-containing tubes using a SpeedMill PLUS cooling homogenizer (Analytikjena, Jena, Germany). Genomic DNA was extracted from each homogenized sample using the BlackPREP Tick DNA/RNA Kit (IST Innuscreen GmbH, Germany) according to the manufacturer's instructions. The extracted DNA was stored at -20 °C until it was used for PCR analysis.

Two separate PCR analyses were performed independently for the cytochrome c oxidase subunit 1 (cox1) and Internal Transcribed Spacer 2 (ITS2) markers. The first PCR was conducted using primers HCO2064 and HCO1215, which amplify an approximately 850 bp region of the mitochondrial cox1 gene. The second PCR used primers 3SA and JB9A, amplifying the nuclear ITS2 gene, covering the entire 1099 bp gene^{41,42}. Each marker was amplified in a single-step conventional PCR reaction. PCR products for each marker were purified using the PureLink™ Quick Gel Extraction Kit (Invitrogen, Thermo Scientific, Lithuania) and sequenced bidirectionally via Sanger sequencing with the BigDye™ Terminator V3.1 Cycle Sequencing Kit (Applied Biosystems, Foster City, CA, USA) on an Applied Biosystems™ 3500 Genetic Analyzer. Raw sequence data from both directions was reviewed, edited in the chromatogram, and assembled into a single sequence. The resulting sequences were subjected to BLAST homology analysis in GenBank (National Center for Biotechnology Information, https://www.ncbi.nlm.nih.gov/genbank) and BOLD (Barcode of Life Data System, http://www.boldsystems.org) databases for nucleotide comparison and similarity assessment.

Genetic diversity, population genetic structure and demographic history

The nucleotide data were organized into two separate datasets: one for the *cox1* gene and one for the ITS2 gene. A concatenated dataset was also created by combining the *cox1* and ITS2 data for each sample. The *cox1* sequences were converted into amino acid (protein) sequences using AliView v1.26⁴³ and were checked for potential stop codons and the presence of *numts* (Nuclear mitochondrial DNA segments, which are fragments of mitochondrial DNA that have been incorporated into the nuclear genome) using BLAST. The *cox1* sequences were aligned as translated amino acids using the MUSCLE algorithm, integrated with AliView software, while the ITS2 sequences were aligned using the Q-INS-i algorithm, which takes secondary structure information into account, with a scoring matrix of 200 PAM/k=2 and a gap opening penalty of 1.53 incorporated into MAFFT v.7⁴⁴.

Nucleotide diversity (π), the number of observed haplotypes/genotypes (h), haplotype/genotype diversity (Hd), the number of segregation sites (S), the average number of nucleotide differences (k), and the distribution of haplotypes/genotypes across populations were calculated using DnaSP v6.12.03⁴⁵ for three datasets: cox1, ITS2, and the concatenated data. Populations were evaluated based on 31 sampling sites, two regions (CN and NE), and a combined dataset representing all samples. The distribution of pairwise sequence divergence was assessed using mismatch distribution analysis in DnaSP, and the formula "Tau = 2ut" was applied to estimate the timing of population size changes^{45,46}. To examine the relationships between haplotypes/genotypes, network analysis was conducted using TCS v1.21⁴⁷ and visualized in tcsBU⁴⁸. Additionally, pairwise distances between haplotypes/genotypes were analyzed in MEGA 11.0.13⁴⁹ under the "p-distance" model with 1,000 bootstrap replicates, and the resulting matrices were visualized with SDT v1.2⁵⁰.

The neutral mutation hypothesis (The neutral theory of molecular evolution, which posits that most evolutionary changes at the molecular level are caused by genetic drift of neutral mutations rather than natural selection) was tested using Tajima's D, Fu's Fs, and Fu and Li's D-F statistics in DnaSP^{45,51,52}. Genetic variance and pairwise genetic differentiation within and among populations were calculated using molecular analysis of variance (AMOVA), performed locus by locus with Arlequin v3.5.2.2 and 1000 replicates⁵³. The significance of covariance components associated with different levels of genetic structure—within populations, within population groups, and between groups—was tested using nonparametric permutation procedures^{53,54}. The fixation index (F_{ST}) was calculated to estimate the amount of pairwise genetic variance explained by population structure, using Wright's F-statistics⁵⁵. Additionally, the population structure was analyzed with group simulations ranging from K=2-10 (three runs for each group) using the Bayesian clustering algorithm with STRUCTURE^{56,57}, and the package "pophelper" on the R platform was used to determine the optimal number of groups from the STRUCTURE outputs with the highest value of Delta K⁵⁸. Mantel and SAMOVA (Spatial Analysis of Molecular Variance) tests were employed to evaluate the correlation between genetic variation and geographic distance^{59,60}. The Mantel test was conducted using the 'geodist', 'ape', and 'vegan' packages in R (v4.3.2, R Core Team 2020) with Pearson's product-moment correlation (r) and statistical significance determined by 1,000,000 permutations^{61,62}. SAMOVA v2.0 software was used with 31 sampling sites, 2-10 group simulations, and 10,000 iterations based on the F_{CT} value obtained⁶⁰.

In our statistical analyses, we utilized AMOVA, F_{ST} calculations, and Bayesian clustering to assess the population structure. We recognize the potential risk of the Wahlund effect, which can cause artificial population subdivisions. To mitigate this, we ensured that our sampling strategy was both broad and representative, covering a wide range of ecological and geographical conditions. This approach minimized the likelihood of sampling individuals from mixed populations, which could lead to confounding results. Additionally, we performed a preliminary analysis to verify the presence of genetic structure before conducting AMOVA and Bayesian clustering, further strengthening the robustness of our findings.

Phylogenetic analysis

Genetic data, including cox1 gene-based haplotypes and ITS2 gene-based genotypes, were used to create the following datasets for phylogenetic analyses:

- a. A dataset comprising *cox1*-based haplotypes identified in this study and *D. raskemensis* (GenBank accession no. MT308586) as an outgroup.
- b. A dataset comprising ITS2-based genotypes identified in this study and *D. raskemensis* (PP618825) as an outgroup.
- c. A concatenated dataset comprising *cox1*+ITS2 (combined) genotypes from this study and *D. raskemensis* (MT308586+PP618825) as an outgroup.
- d. A dataset comprising *cox1*-based haplotypes from this study and *cox1* sequences from species in the subgenus *Serdjukovia* (*D. marginatus*, *D. raskemensis*, *D. niveus*, *D. silvarum*, and *D. nuttalli*) registered in the GenBank, with *D. reticulatus* (MT478096, OM142141, and OQ947121) as an outgroup.
- e. A dataset comprising ITS2-based genotypes from this study and ITS2 sequences of species in the subgenus *Serdjukovia* registered in the GenBank, with *D. reticulatus* (OR428530, S83080, and OM142152) as an outgroup.

The reliability of the sequences in each dataset was assessed individually using GUIDANCE2⁶³. Unreliable sequences or columns (in protein-coding genes) were eliminated based on GUIDANCE2 outputs, improving the quality of the phylogenetic trees. The *cox1* datasets were aligned as translated amino acids using the MUSCLE algorithm⁶⁴, while the ITS2 datasets were aligned using the MAFFT algorithm⁴⁴. The overall mean distance (*p*-distance) was calculated in MEGA 11.0.13⁴⁹ to assess alignment reliability and average identity. Best-fit nucleotide substitution models were selected using the Bayesian Information Criterion (BIC) in jModelTest 2.1.10⁶⁵ and ModelTest-NG 0.1.6⁶⁶. Phylogenetic analyses were conducted using a Markov chain Monte Carlo (MCMC) integration method based on Bayesian inference using software in the BEAST2 package (BEAUti v2.7.6, BEAST v2.7.6, TreeAnnotator v2.7.4)⁶⁷. The MCMC chain was run for 100 million generations, and the ESS values obtained were checked in Tracer v1.7.2. software⁶⁸. The final phylogenetic tree was generated in TreeAnnotator (2.7.4), after excluding the first 20% of trees as burn-in. The trees were visualized in FigTree v1.4.4 (Rambaut, A. University of Edinburgh, Edinburgh, UK; http://tree.bio.ed.ac.uk/software/figtree) and rooted using the included outgroup. Branch support was evaluated based on posterior probabilities from BEAST. Phylogenetic clades were named according to species and haplogroups/genogroups, and low-support branches were collapsed in the final trees.

Mapping and database registration of haplotypes and genotypes

Distribution maps of the characterized *D. marginatus* haplotypes and genotypes were generated using ArcGIS 10.6.1 (Esri, 2018) with base maps at various resolution levels. The genetic and barcode data were registered in the NCBI and BOLD databases. Specifically, the *cox1* data for *D. marginatus* haplotypes, including necessary barcode information (such as images and geographical coordinates), were uploaded to the BOLD system, with haplotypes achieving 100% barcode compliance. Furthermore, both *cox1* and ITS2 data for *D. marginatus* haplotypes and genotypes were deposited in the GenBank database, each assigned specific accession numbers.

Results

A total of 938 (360&3, 578QQ) host-seeking adult *D. marginatus* individuals were collected from 151 pinpoint locations across 31 sampling sites. This included 553 individuals from 102 locations within 19 sampling sites in

CN and 256 individuals from 49 locations within 12 sampling sites in NE. All individuals were classified into the *D. marginatus* complex based on morphological criteria and identified as the *D. marginatus* morphotype. For the population genetics analysis, a total of 361 *D. marginatus* individuals (16833, 19399) were selected from 31 sampling sites, with each site contributing between 8 and 21 individuals. Additionally, to ensure broad ecological and geographical coverage, at least one tick was collected from each of the 150 locations. However, the primary focus of this study is not on individual locations, but rather on the genetic differentiation between sampling sites and the two major regional populations: CN (n=226) and NE (n=135). Given this approach, the sample size is considered sufficient for assessing regional population structure. Detailed information about the collected tick specimens included in the genetic analysis is provided in Table 1 and Table S2, and their geographical distribution is illustrated in Fig. 1.

All *D. marginatus* samples included in the population genetics were subjected to PCR amplification of the partial *cox1* and the entire ITS2 gene, as outlined in the methodology. Positive amplicons of the expected sizes were successfully obtained for all samples. The sequences from these amplicons were assembled bidirectionally, and after eliminating low-quality regions at the beginning and end, the final *cox1* sequence had an average length of 840 bp. For the ITS2 gene, a complete sequence of 1099 bp was obtained. Additionally, to be used as an outgroup and for phylogenetic analysis, the entire ITS2 gene region of *D. raskemensis* was sequenced. Although *cox1* data for *D. raskemensis* (GenBank accession MT308586) were already available, ITS2 data were absent in the GenBank database. Thus, ITS2 sequencing was performed on the same specimen from our DNA bank, and the resulting sequence was deposited in GenBank under the accession number PP618825.

Study region	Sampling site	Total number of specimens obtained (gender)	Number of locations where samples were collected	Number of samples included in population genetics (Gender)	Number of locations from which samples included in population genetics were obtained
CN	L1	28 (10 ්, 18♀)	9	12 (5♂, 7♀)	9
CN	L2	17 (10♂, 7♀)	6	12 (7♂, 5♀)	6
CN	L3	22 (8♂, 14♀)	6	13 (6♂, 7♀)	6
CN	L4	25 (10♂, 15♀)	6	12 (6♂, 6♀)	6
CN	L5	24 (5♂, 19♀)	6	21 (43, 179)	5
CN	L6	47 (16♂, 31♀)	8	14 (78, 79)	8
CN	L7	32 (10გ, 22♀)	6	12 (5♂, 7♀)	6
CN	L8	38 (19♂, 19♀)	6	12 (6♂, 6♀)	6
CN	L9	27 (10♂, 17♀)	6	12 (5♂, 7♀)	6
CN	L10	19 (5♂, 14♀)	6	12 (5♂, 7♀)	6
CN	L11	42 (16♂, 26♀)	8	12 (6♂, 6♀)	8
CN	L12	22 (7♂, 15♀)	3	12 (63, 69)	3
CN	L13	28 (17♂, 11♀)	4	12 (5♂, 7♀)	4
CN	L14	41 (16♂, 25♀)	5	12 (6♂, 6♀)	5
CN	L15	20 (5♂, 15♀)	3	12 (5♂, 7♀)	3
CN	L15B	17 (2♂, 15Q)	3	8 (2층, 6♀)	3
CN	LA	30 (13გ, 17Չ)	2	10 (6♂, 4♀)	2
CN	LGr	45 (21♂, 24♀)	5	8 (43, 42)	5
CN	LM	29 (11♂, 18♀)	4	8 (43, 42)	4
NE	L16	23 (12♂, 11♀)	5	12 (7♂, 5♀)	5
NE	L17	18 (8♂, 10♀)	3	12 (6♂, 6♀)	3
NE	L18	18 (9♂, 9♀)	4	12 (8♂, 4♀)	4
NE	L19	30 (14♂, 16♀)	2	12 (5♂, 7♀)	2
NE	L20	23 (5♂, 18♀)	5	13 (4♂, 9♀)	5
NE	L21	45 (13♂, 32♀)	7	16 (8♂, 8♀)	7
NE	L22	23 (13♂, 10♀)	2	12 (7♂, 5♀)	2
NE	L23	10 (2♂, 8♀)	2	10 (2♂, 8♀)	2
NE	L24	27 (12♂, 15♀)	6	12 (7♂, 5♀)	6
NE	L25	20 (13♂, 7♀)	1	8 (6♂, 2♀)	1
NE	L26	31 (9♂, 22♀)	5	8 (43, 49)	5
NE	L27	117 (42♂, 75♀)	7	8 (43, 49)	7
Total	31	938 (363♂, 575♀)	151	361 (1688, 1939)	150

Table 1. Data on *D. marginatus* specimens collected and subjected to genetic analysis. CN: Central Anatolia, NE: Northeast Anatolia.

Population structure and demographic history based on the cox1 gene

The cox1 sequences of 361 characterized individuals were aligned as amino acids using the MUSCLE algorithm and trimmed to match the shortest sequence, resulting in a dataset of sequences with a total length of 824 bp. As the cox1 gene is protein-coding, the nucleotide sequences were also translated into amino acid sequences and analyzed for the presence of stop codons and numts. No stop codons or numts were detected in any of the sequences. Analyses were performed separately for each sampling site, as well as for the two regional groups and the overall population. However, it was determined that the results were more informative when analyzed on a regional basis, so most inferences were drawn from the analyses of the two regions and the entire population combined.

Central Anatolia (CN)

In the CN, 71 haplotypes were identified, with 67 of which (CX-CN1-67) were unique to this region, while four haplotypes (CX-CNNE1-4) were shared between regions. Among these, 49 individuals were represented by a single haplotype, while the remaining samples were grouped into haplotypes with multiple representatives. Neutrality tests revealed negative and statistically significant values for Tajima's D and Fu and Li's D and F (P<0.02), while the Fu's Fs value was also negative (Table 2). The mismatch distribution analysis displayed a unimodal pattern (Fig. S1).

Northeast Anatolia (NE)

In the NE, 64 haplotypes were identified, including 60 unique haplotypes (CX-NE1-60) that are specific to this region and four haplotypes (CX-CNNE1-4) shared between regions. Among these, 49 individuals were represented by a single haplotype, while the remaining individuals were grouped into haplotypes with multiple representatives. Neutrality tests showed that Tajima's D, Fu and Li's D and F values were negative and statistically significant (P < 0.02), and Fu's Fs value was also negative (Table 2). The mismatch distribution analysis revealed a unimodal pattern (Fig. S1).

All regions (ALL)

When all study areas were considered as a single population, a total of 131 haplotypes were identified. Of these, 67 were specific to CN, 60 to NE, and four were shared between the two regions, accounting for all haplotypes detected in the study. Among the samples, 98 individuals were represented by a single haplotype, while the remaining samples were grouped into haplotypes with multiple individuals. Neutrality tests showed that Tajima's D, Fu and Li's D and F values were negative and statistically significant (P < 0.02), and Fu's Fs value was also negative (Table 2). The mismatch distribution analysis exhibited a unimodal pattern (Fig. S1). Additionally, the results of the analysis of polymorphic regions are presented in Table S3, based on both the total population (all combined samples) and the two regional populations (CN and NE).

Genetic differentiation and population structure

To determine genetic variance and pairwise genetic differentiation (F_{ST}) at the cox1 gene level, populations were categorized into 31 sampling sites and two regional populations. AMOVA was performed locus by locus. In the dataset with 31 populations, genetic variation among populations accounted for 15.94%, while within-population variation was 84.07%, yielding an F_{ST} value of 0.15936 (P < 0.001). In the two regional populations, genetic variation among populations was 19.35%, while variation within populations was 80.64%, with an F_{ST} value of 0.19353 (P < 0.001) (Table S4). The most differentiated population, with the highest F_{ST} value (0.41205, P < 0.001), was found between sampling site L6 in CN and L16 in NE. A distance matrix and color plot generated from the F_{ST} values for the 31 populations are provided in the supplementary files (Fig. S2 and Table S5).

STRUCTURE analyses were conducted with simulations ranging from K=2 to 10 groups (27 simulations in total, three simulations for each group). The most appropriate number of groups was determined to be K=3 using pophelper (Fig. S3), and the population was evaluated based on three distinct ancestral groups. This analysis revealed significant population structure between the CN and NE populations of *D. marginatus*. The STRUCTURE graph indicated that red alleles were predominant in the CN population, while green alleles dominated in the NE population, with black alleles being rare and recessive in both regions (Fig. 2A). The correlation between genetic variation and geographic distance was assessed using the Mantel test on the dataset of 361 *D. marginatus* individuals, based on cox1 gene sequences and individual geographical coordinates. The test yielded a statistically significant result (r=0.2785, P<0.05). Additionally, the dataset, with geographical coordinates based on 31 sampling sites, was subjected to SAMOVA analysis. Simulations from K=2 to 10

Population	n	h	Hd	π	S	k	Fu's Fs	Tajima's D	Fu and Li's D	Fu and Li's F
CN	226	71	0.856	0.00213	66	1.759	-33.24	-2.52098****	-6.80672***	-5.82993***
NE	135	64	0.926	0.00411	64	3.387	-34.098	-2.22418***	-5.46808***	-4.89132***
ALL	361	131	0.9283	0.00319	102	2.629	-32.694	-2.47266****	-7.36873***	-5.91534***

Table 2. *Cox1* gene-based population genetics of Anatolian populations of *D. marginatus*. CN: Central Anatolian population, NE: Northeast Anatolian population, ALL: All population. n = number of individuals, h = number of haplotypes, Hd = haplotype diversity, π = nucleotide diversity, S = number of segregation sites, and k = average number of nucleotide differences. *** Statistically significant (P<0.02), **** Statistically significant (P<0.001).

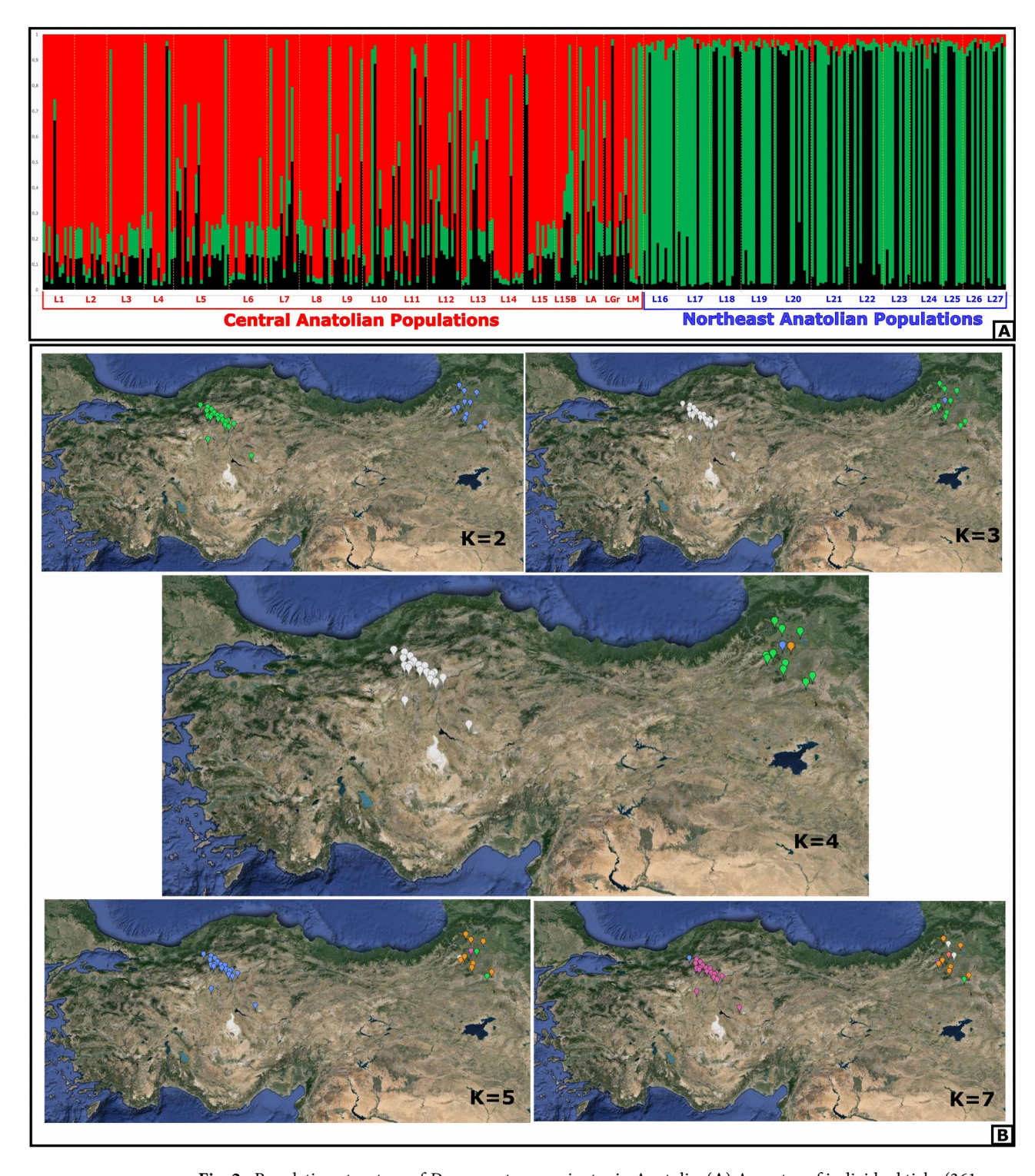


Fig. 2. Population structure of *Dermacentor marginatus* in Anatolia. (**A**) Ancestry of individual ticks (361 Anatolian *D. marginatus* individuals from 150 sites) assuming *K* cluster of genetic similarity, based on the results of STRUCTURE analyses using cox1 gene (K=3). The first 19 sampling sites (L1-LM) contain samples from the CE population and the remaining locations groups (L16-27) contain samples from the NE population. Each bar corresponds to a tick specimen, vertical dashed yellow lines indicate the boundaries between sampling sites, and the vertical axis represents the membership probability of an individual to each cluster. (**B**) Maps showing genetic clusters of *D. marginatus* individuals (n=361) according to 31 sampling sites, based on the results of SAMOVA using cox1 gene. The value K refers to the number of simulated groups. Satellite images were processed using SAMOVA 2.0 software.

groups were performed, with K=4 being identified as the most appropriate based on the F_{CT} value. In the K=2 simulation, the entire population was divided into two separate groups: CN and NE populations. As the number of groups increased up to K=7, separations were observed within the NE populations, while the CN population remained as a single group. At K=7, LGr from CN was the first to separate. At K=4, the CN population formed a single group, while the NE population was divided into three groups: Group 1: L17; Group 2: L18, L19, L20, L21, L22, L23, L24, L25, L26, L27; Group 3: L16 (Fig. 2B).

Haplotype distribution, Haplotype network, and Pairwise-Distance

The 131 characterized *D. marginatus* individuals were represented by 131 distinct haplotypes based on the *cox1* gene. Among these, 67 haplotypes were unique to CN, 60 haplotypes were specific to NE, and four haplotypes were shared between the two regions. In CE, the most common haplotype, CX-CN3, was represented by 77 individuals, followed by CX-CN2 with 35 individuals, and other haplotypes with progressively fewer individuals. The CX-CN3 haplotype was present in all sampling sites in CN, while CX-CN2 was found in all but three sampling sites (L7, LA, and LGr).

In NE, the most common haplotype was CX-NE15, represented by 10 individuals, followed by CX-NE1 with six individuals. These haplotypes were distributed across specific sampling sites, such as CX-NE15, which was found in L18, L20, L21, L22, and L27, and CX-NE1, found in L16, L18, L21, and L22. The shared haplotypes, CX-CNNE1, CX-CNNE3, CX-CNNE2, and CX-CNNE4, exhibited varying distribution patterns, with CX-CNNE1 being the most abundant, found in eight sampling sites in CN and across all sampling sites in NE. Detailed information on the haplotypes and their distribution across the different sampling sites is provided in Table S6 and illustrated in Fig. 3.

A pairwise-distance analysis was performed using the 131 identified haplotypes. The most genetically distant haplotype was CX-NE53, represented by a single individual (Dm-2411) from sampling site L24 in NE. Intraspecific genetic variation ranged from 0.12% to 1.94%, with noticeable pairwise differentiation between region-specific haplotypes. Genetic differentiation was more pronounced within haplotypes from the NE (Table S7 and Fig. 3).

The 131 characterized haplotypes were analyzed for genetic similarity and haplotype specificity using BLAST and identification analyses in both the GenBank and BOLD databases. In the GenBank database, the haplotypes could be compared with sequences of equal size, while in the BOLD database, comparisons were made with sequences that were, on average, at least 200 bp shorter than our haplotypes. Therefore, similarity and uniqueness analyses were based on BLAST results. According to the BLAST analysis, none of the haplotypes were identical to any existing records (whether through full or close length comparisons), confirming that all 131 haplotypes were unique. The most similar sequences, with homologies ranging from 98.30% to 99.88% (comparison rate above 98%), were found to be from *D. marginatus* in Kazakhstan (MN907848 and OQ415364), Slovakia (MK905212), and China (NC_062069 and OM368304). While comparison rates in the BOLD database were generally low, identification analysis showed 99.38% to 100% similarity with *D. marginatus* records under the AAL1447 BOLD accession, primarily from Spain, Romania, Croatia, and Georgia (Table S8).

Population structure and demographic history based on the ITS2 gene

The complete ITS2 gene sequence (total length: 1099 bp) of 361 characterized *D. marginatus* individuals was aligned using the MAFFT algorithm. Comparisons within the dataset revealed no insertions or deletions among the sequences. Analyses were conducted separately for each sampling site, as well as at the levels of two regions and the entire population.

Central Anatolia (CN)

In the CN, 65 genotypes were identified, comprising 37 region-specific genotypes (IT-CN1-37) and 28 common genotypes (IT-CNNE1-28). Among these, 33 individuals were represented by a single genotype, while the remaining samples were grouped into genotypes shared by multiple individuals. Neutrality tests revealed mixed results: Tajima's D was positive and statistically insignificant, Fu and Li's D was positive but statistically significant (P < 0.05), Fu and Li's F was negative and statistically insignificant, and Fu's Fs was negative (Table S9). The mismatch distribution analysis exhibited a unimodal-like pattern (Fig. S4).

Northeast Anatolia (NE)

In the NE, 67 genotypes were identified, including 39 region-specific genotypes (IT-NE1-39) and 28 common genotypes (IT-CNNE1-28). Among these, 36 individuals were represented by a single genotype, while the remaining samples were grouped into genotypes shared by multiple individuals. Neutrality tests showed that Tajima's D was negative but statistically insignificant, while Fu and Li's D and F values were negative and statistically significant (P < 0.05). Additionally, Fu's Fs was negative (Table S9). The mismatch distribution analysis revealed a unimodal pattern (Fig. S4).

All regions (ALL)

When all study areas were considered as a single population, 104 genotypes were identified. Among these, 37 genotypes were specific to CN, 39 were specific to NE, and 28 were shared between the two regions. Of the samples, 99 individuals were represented by a single genotype, while the remaining individuals were grouped into genotypes shared by multiple samples. Neutrality tests indicated that Tajima's D was negative but statistically insignificant, while Fu and Li's D and F values were negative and statistically significant (P < 0.02), and Fu's Fs was also negative (Table S9). The mismatch distribution analysis produced a unimodal-like pattern (Fig. S4). Additionally, the analysis of polymorphic regions was conducted both for the combined population and for the two regional populations, with detailed results presented in Table S10.

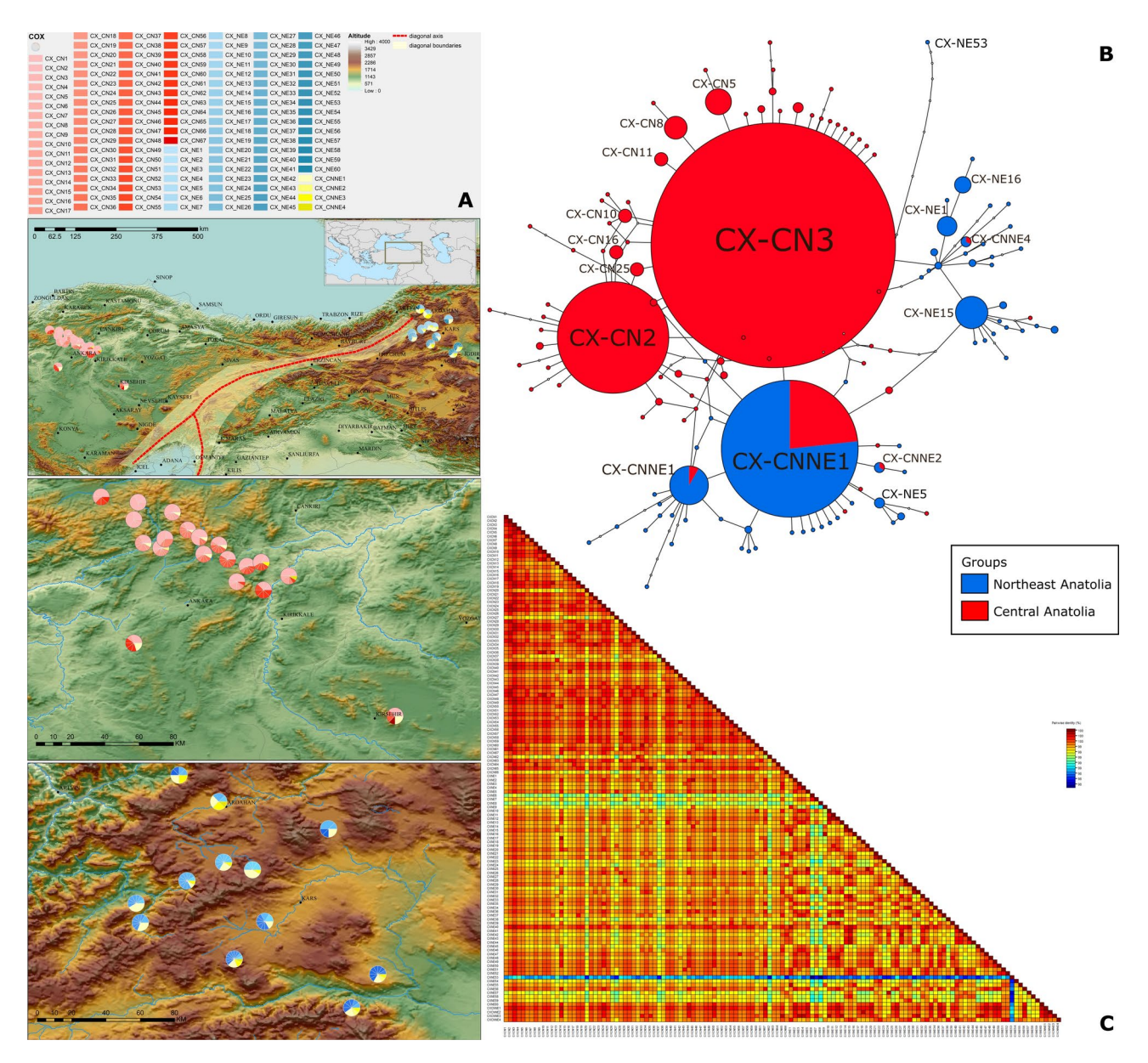


Fig. 3. Haplotype distribution, network and pairwise distances of *Dermacentor marginatus* (n = 361) based on cox1 gene. (**A**) Distribution map of haplotypes according to sampling sites. The CN haplotypes are colored in shades of red, the NE haplotypes in shades of blue and shared haplotypes in shades of yellow. (**B**) TCS network tree of haplotypes. Individuals from CN are colored in red, while individuals from the NE in blue. The names of major haplotypes with multiple samples are indicated on the tree. (**C**) Color coded matrix of pairwise similarity scores belonging to haplotypes. Maps were generated using ArcGIS 10.6.1 software.

Genetic differentiation and population structure

To assess genetic variance and pairwise genetic differentiation (F_{ST}) at the ITS2 gene level, populations were grouped into 31 sampling sites-based and two regional populations. AMOVA was performed locus by locus. In the dataset with 31 sampling sites, genetic variation among populations accounted for 7.31%, while within-population variation was 92.69%, resulting in an F_{ST} value of 0.07309 (P < 0.01). In the dataset divided into two regions, genetic variation among populations was calculated at 2.97%, while within-population variation was 97.03%, with an F_{ST} value of 0.02966 (P < 0.001) (Table S11). The most genetically differentiated populations, with the highest F_{ST} value (0.3188, P < 0.001), were observed between L10 in CN and L22 in NE. The distance matrix and color plot based on F_{ST} values for the 31 populations are provided in the supplementary materials (Fig. S5 and Table S12).

STRUCTURE analyses were performed with simulations ranging from K=2 to 10 groups (27 simulations total, with three runs per group). The most appropriate group number was determined to be K=2 using pophelper, with K=3 (the second highest delta K) also considered for evaluation (Fig. S6). Results were assessed based on both two and three ancestral groups. When the simulation was based on two ancestral groups using

the ITS2 gene, no distinct population structuring was observed at either the sampling site or regional level. However, the simulation with three ancestral groups revealed weak population structuring based on study regions, though it was less pronounced compared to the results from the cox1 gene (Fig. S7). The correlation between genetic variation and geographical distance was evaluated using the Mantel test for 361 D. marginatus individuals characterized by the ITS2 gene with individual geographical coordinates. The test yielded an r-value of 0.04177, which was statistically significant (P < 0.05). Additionally, SAMOVA analysis was conducted on the same dataset using geographical coordinates grouped into 31 sampling sites. Simulations from K=2 to 10 groups were performed, with K=4 determined as the most appropriate group simulation based on the F_{CT} value, although all groups were evaluated. At K=4, sampling sites were not geographically segregated strictly by region. Instead, one group consisted of samples from nine sampling sites in CN (Group 1: L1, L3, L6, L4, L8, L10, L11, L12, and L15). Another group formed from a single location in NE (Group 2: L16), and a third group also in NE (Group 3: L18). A fourth, shared group (Group 4) included samples from 20 sampling sites across both CN and NE (L2, L5, L7, L9, L13, L14, L15B, LA, LGr, LM, L17, L19, L20, L21, L22, L23, L24, L25, L26, and L27) (Fig. S8).

Genotype distribution, Genotype network, and Pairwise-Distance

The 104 characterized *D. marginatus* genotypes based on the ITS2 gene were distributed as follows: 37 genotypes unique to CN, 39 unique to NE, and 28 shared between regions. Among the CN-specific genotypes, IT-CN7 was the most common, represented by three individuals, while IT-CN6, IT-CN9, and IT-CN16 were each represented by two individuals; the remaining genotypes were represented by a single individual. In NE, IT-NE20, IT-NE27, and IT-NE37 were each represented by two individuals, with all other genotypes represented by single individuals. For the 28 shared genotypes, IT-CNNE5 was the most abundant, represented by 56 individuals across most sampling sites, except L3, L13, L16, and L24. This was followed by IT-CNNE1 (30 individuals) and IT-CNNE2 (23 individuals) in various sampling sites. Other notable shared genotypes, such as IT-CNNE8 (20 individuals), IT-CNNE13 (19 individuals), and IT-CNNE9 (16 individuals), displayed varying degrees of distribution across CN and NE. The remaining shared genotypes were represented by fewer individuals, typically across limited sampling sites. Detailed information on the genotypes and their distributions across the different sampling sites is presented in Table S13 and Fig. S9.

Å pairwise-distance analysis was performed using the 104 identified genotypes. The most genetically distant genotypes were IT-CN28 from CN and IT-NE29 from NE. IT-CN28 was represented by a single individual (Dm-13910) from location L13, while IT-NE29 was represented by a single individual (Dm-2421) from location L24. Intraspecific genetic variation ranged from 0.09% to 1.55%, with partial pairwise differentiation observed among region-specific genotypes. Notably, genetic differentiation within NE genotypes was slightly more pronounced compared to CN. However, this differentiation was less distinct than that observed in the *cox1* gene (Table S14 and Fig. S9).

The 104 characterized genotypes were analyzed for genetic similarity and specificity using BLAST. The analysis confirmed that none of the genotypes had identical matches in existing records (based on full or nearfull length comparisons), establishing that all 104 genotypes were unique. Among the most similar sequences, with homologies ranging from 98.36% to 99.91%, were *D. marginatus* records from Romania (FN296269, FN296278, FN296273, FN296275), Iran (GQ144707), and Germany (S83081), as well as sequences of closely related species, such as *D. niveus* from Iran (GQ144706) and *D. silvarum* from China (JQ737110) (Table S15).

Population structure and demographic history based on the *cox1*+ITS2 concatenated dataset

The *cox1*+ITS2 concatenated dataset (total length: 1923 bp) of 361 characterized *D. marginatus* individuals was aligned using the MAFFT algorithm. Comparisons within the dataset revealed no insertions or deletions. Analyses were performed separately for each sampling site, as well as at the regional level (CN and NE) and for the entire population dataset.

Central Anatolia (CN)

In the CN, 153 genotypes were identified, consisting of 149 region-specific genotypes (CNC-CN1-149) and four common genotypes (CNC-CNNE1-4) shared between regions. Among the samples, 129 individuals were represented by a single genotype, while the remaining individuals were grouped into genotypes shared by multiple samples. Neutrality tests revealed that Tajima's D and Fu and Li's D and F values were negative and statistically significant (P < 0.05), while Fu's Fs was also negative (Table S16). The mismatch distribution analysis showed a unimodal pattern (Fig. S10).

Northeast Anatolia (NE)

In the NE, 129 genotypes were identified, including 125 region-specific genotypes (CNC-NE1-125) and four common genotypes (CNC-CNNE1-4) shared between regions. Among the samples, 121 individuals were represented by a single genotype, while the remaining individuals were grouped into genotypes shared by multiple samples. Neutrality tests showed that Tajima's D was negative but statistically insignificant, while Fu and Li's D and F values were negative and statistically significant (P < 0.05), and Fu's Fs was also negative (Table S16). The mismatch distribution analysis resulted in a unimodal graph (Fig. S10).

All regions (ALL)

When all study areas were considered as a single population, 278 genotypes were identified. Of these, 149 genotypes were specific to CN, 125 were specific to NE, and four genotypes were shared between the two regions. Among the samples, 250 individuals were represented by a single genotype, while the remaining individuals were grouped into genotypes that were shared by multiple samples. Neutrality tests indicated that Tajima's D

and Fu and Li's D and F values were negative and statistically significant (P < 0.02), while Fu's Fs was negative (Table S16). The mismatch distribution analysis showed a unimodal pattern (Fig. S10). Additionally, the results from the analysis of polymorphic regions, considering both the combined population and the two regional populations, are presented in Table S17.

Population structure

To assess genetic variance and pairwise genetic differentiation (F_{ST}) within and between populations using the concatenated dataset, populations were categorized into 31 sampling sites-based and two regional populations. AMOVA was performed locus by locus. In the dataset with 31 populations, the genetic variation among populations was 10.51%, while within-population variation was 89.49%, resulting in an F_{ST} value of 0.10511 (P<0.001). In the dataset based on two regions, genetic variation among populations was 9.4%, and within-population variation was 90.6%, with an F_{ST} value of 0.09396 (P<0.001) (Table S18). The most differentiated population, with the highest F_{ST} value (0.28249, P<0.001), was found between L14 in CN and L16 in NE. The F_{ST} distance matrix and color plot based on the 31 populations are provided in the supplementary files (Fig. S11 and Table S19).

STRUCTURE analyses were performed with simulations ranging from K=2 to 10 groups (27 total simulations, three for each group). The optimal number of groups was determined to be K=2 using pophelper, with K = 3 also considered due to the second highest delta K value (Fig. S12). The results were evaluated for both two and three ancestral groups. The simulation based on K=2 showed less pronounced population structuring at both the sampling site and regional levels, based on the concatenated dataset. However, when K=3 was used, regional population structuring became evident, though weaker than that observed for the cox1 gene (Fig. S13). To assess the correlation between genetic variation and geographical distance, a Mantel test was conducted on the dataset of 361 D. marginatus individuals, using individual geographical coordinates. The test yielded a statistically significant r-value of 0.1863 (P<0.05). Additionally, SAMOVA analysis was performed with geographical coordinates based on 31 sampling sites. Simulations from K=2 to 10 were carried out, with K=5determined as the most appropriate based on the F_{CT} value. This simulation revealed that, at K=2, CN and NE were separated into two distinct groups. As the number of groups increased, separations were observed within the NE populations, while CN populations remained as a single group. From K=6 onward, locations L9 and L14 were the first to separate from CN. At K=5, the CN populations formed a single group, while the NE populations were divided into four groups: Group 1 (L17), Group 2 (L18), Group 3 (L19, L20, L21, L22, L23, L24, L25, L26, L27), and Group 4 (L16) (Fig. S14).

Genotype distribution, genotype network, and pairwise-distance

A total of 278 genotypes were identified in the characterized *D. marginatus* individuals based on the concatenated dataset. Among these, 149 genotypes were specific to CN, 125 genotypes were specific to NE, and four genotypes were shared between both regions. The genotypes from CN included the most common CNC-CN10, which was represented by nine individuals across multiple sampling sites (L1, L5, L8, L9, L10, L12, L15B, LGr), and CNC-CN14, which was also represented by nine individuals but across different locations (L2, L3, L4, L5, L6, L11, L12, L15). Other notable genotypes in this region were CNC-CN13, represented by eight individuals, and CNC-CN22, represented by seven individuals, among others. The remaining genotypes from CN were represented by fewer individuals, with some found in specific locations and others by just a single individual. In NE, the genotypes were similar, with the most common being CNC-NE9, CNC-NE38, and CNC-NE53, each represented by two individuals in specific sampling sites. The majority of the genotypes in NE were represented by one individual. The shared genotypes between CN and NE included CNC-CNNE2, represented by six individuals in multiple sampling sites, and CNC-CNNE1, which was found in three individuals across L3, L10, and L16, while other common genotypes showed variations across both regions. Detailed information on these genotypes and their distribution across the different sampling sites can be found in Table S20.

Pairwise-distance analysis was performed using the 278 genotypes identified in this study. Among these genotypes, the most genetically distant were CNC-NE93, CNC-NE94, CNC-NE15, and CNC-NE16, all of which were found in NE. Specifically, the CNC-NE93 and CNC-NE94 genotypes were represented by a single individual each in sampling site L24 (Dm-2411 and Dm-2421), while CNC-NE15 and CNC-NE16 genotypes were represented by single individuals in sampling site L17 (Dm-1714 and Dm-1721). The intraspecific genetic variation ranged from 0.05% to 1.20%, and pairwise differentiation among region-specific genotypes was observed, particularly in NE, where the differentiation within genotypes was more pronounced. These findings highlight regional genetic variation, and further details on the pairwise distance analysis can be found in Table S21 and Fig. S15.

Phylogenetic relationship

Cox1 phylogeny

A dataset including 131 *D. marginatus* haplotypes based on the *cox1* gene was created, along with specimens recorded as *D. marginatus*, *D. niveus*, *D. raskemensis*, *D. nuttalli*, and *D. silvarum* in the subgenus *Serdjukovia* from the GenBank database. Additionally, three *D. reticulatus* specimens (MT478096, OM142141, and OQ947121), classified under a different subgenus of *Dermacentor*, were used as outgroups. After performing reliability analysis to remove duplicate sequences and ensure minimum length, the dataset was edited and aligned. The final dataset consisted of sequence data for a total of 281 samples (comprising 131 haplotypes, 147 GenBank records, and 3 outgroups) (Table S22).

The constructed phylogenetic tree revealed three main clades: *D. marginatus*, *D. raskemensis*, and *D. silvarum/nuttalli*, all supported by high posterior probabilities (Fig. 4). Within the *D. marginatus* clade, at least five haplogroups and three well-supported branches (posterior = 0.82–1) were identified, including 201



Fig. 4. Phylogenetic tree based on Bayesian inference under the TN93(TrN) + Γ + I model using *cox1* data from 201 *Dermacentor marginatus* (131 haplotypes characterized in this study + 71 GenBank records), 53 *D. nuttalli*, 15 *D. silvarum*, eight *D. niveus* and one *D. raskemensis* sequence. *D. reticulatus* sequences (MT478096, OM142141 and OQ947121) were used as outgroup. The node labels refer to the posterior probability and are omitted below the value 0.5. The haplotype characterized in this study is indicated in red and the determined main clades are indicated on the roots.

D. marginatus and seven D. niveus haplotypes. Haplogroup Dm1 was split into two subclades, with subclade Dm1a consisting of 44 haplotypes from this study (40 from NE, two from CN, and two common haplotypes) along with 23 D. marginatus haplotypes from Europe, Asia, and North Africa (Romania, Hungary, Croatia, Slovakia, France, Italy, Germany, China, Kazakhstan, and Tunisia). Subclade Dm1b included 86 haplotypes from this study (65 from CN, 19 from NE, and two common haplotypes) and 12 D. marginatus haplotypes from Europe, Asia, and North Africa (Romania, Croatia, Portugal, Türkiye, Iran, and Tunisia). The phylogenetic tree further revealed that haplogroup Dm2 consisted of a single haplotype from this study (CX-NE53) and 10 D. marginatus haplotypes from China and Kazakhstan. Haplogroup Dm3 included 14 D. marginatus haplotypes from Kazakhstan, China, and Russia. Haplogroup Dm4 comprised seven D. marginatus and seven D. niveus haplotypes from China and Kazakhstan, while haplogroup Dm5 consisted of two D. marginatus haplotypes from China and Kazakhstan. In addition, the D. marginatus main clade contains three separate branches supported by high posterior probabilities (posterior = 0.82-1) and including one haplotype each from Kazakhstan, Pakistan, and Iran. The D. raskemensis clade, with high posterior probability (posterior = 0.98), was divided into two subclades: one derived from a reference sequence of D. raskemensis from Türkiye (MT308586) and the other from a D. niveus sequence from Iran (MK863423). Finally, the D. silvarum/nuttalli main clade, which was highly supported (posterior = 0.98-1) and comprised 68 specimens, was divided into at least five distinct haplogroups. Haplogroup Dns1 included 23 sequences, comprising 16 D. nuttalli and seven D. silvarum haplotypes from China. Haplogroup Dns2 consisted of 29 D. nuttalli and six D. silvarum haplotypes from China, Mongolia, and Russia, while haplogroup Dns3 contained four D. nuttalli and two D. silvarum haplotypes from China. Haplogroup Dns4 comprised two D. nuttalli haplotypes from China, and haplogroup Dns5 contained two D. nuttalli haplotypes from China (Fig. 4 and Table S22).

Upon examining the phylogenetic positions of the haplotypes characterized in this study, the phylogenetic tree revealed that all haplotypes, except for CX-NE53, cluster into two subclades of haplogroup Dm1 alongside

D. marginatus haplotypes from Europe, Asia, and North Africa. The haplotype CX-NE53, obtained from sampling site L24 in NE, clustered into haplogroup Dm2 alongside D. marginatus haplotypes from China and Kazakhstan. This haplogroup is monophyletic with haplogroup Dm3, another Central Asia-related haplogroup, supported by a maximum posterior probability (Fig. 4). The apparent separation of CX-NE53 from the other major haplogroup was further confirmed in a phylogenetic tree that included only the haplotypes from this study (Fig. S16a). Moreover, within the D. marginatus main clade, D. niveus records were found to cluster into a single haplogroup (Dm4), though these did not form a distinct group with strong posterior probability support. Notably, a single additional D. niveus record clustered with the D. raskemensis main clade, being monophyletic with the reference D. raskemensis specimen at maximum posterior probability. The phylogenetic relationship of two other closely related species in the subgenus Serdjukovia, D. nuttalli and D. silvarum, showed that the D. silvarum/nuttalli main clade divides into two clades: D. nuttalli only and D. nuttalli+D. silvarum, with strong posterior probability support. Further analysis revealed that the mixed group further splits into four clades with very high posterior probabilities (posterior=0.98-1), where one clade consists solely of D. nuttalli individuals, while the remaining three contain records for both species (Fig. 4).

ITS2 phylogeny

The ITS2 dataset was constructed to include 104 *D. marginatus* genotypes characterized in this study, along with ITS2 sequence data from closely related taxa within the subgenus *Serdjukovia* (*D. marginatus*, *D. niveus*, *D. raskemensis*, *D. nuttalli*, and *D. silvarum*) retrieved from GenBank. To root the phylogenetic tree, ITS2 sequences from *D. reticulatus* (OM142152, OR428530, and S83080) were incorporated as outgroup sequences. The dataset was curated to remove duplicate sequences and align minimum lengths to match the study's genotypes. After reliability checks, the final dataset consisted of 268 sequences (104 genotypes from this study, 161 sequences from GenBank, and 3 outgroup sequences). Bayesian inference phylogeny was conducted using the GTR+ Γ model, identified as the optimal nucleotide substitution model for this dataset. The resulting phylogenetic tree was rooted using the designated outgroup sequences for proper evolutionary context. Details of the sequences used here are available in Table S23.

The phylogenetic analysis, after collapsing branches with low posterior probabilities, identified three main clades: D. marginatus, D. raskemensis, and D. silvarum/nuttalli. These were supported by high posterior probabilities, alongside one additional D. silvarum/niveus clade with low posterior support (Fig. S17). Within the D. marginatus main clade, two genogroups (DmIT1 and DmIT2) and one branch were identified, all supported by maximum posterior probabilities. This clade includes a total of 132 sequences: 128 D. marginatus, three D. niveus, and one D. silvarum. The largest genogroup, DmIT1, comprises 104 genotypes from this study, 20 D. marginatus genotypes from Iran, China, Romania, and Germany, two D. niveus genotypes from Iran and China, and one D. silvarum genotype from China. Additionally, a single D. marginatus genotype from China (D. marginatus isolate XJ058, KC203417) formed a distinct branch, monophyletic with DmIT1. Genogroup DmIT2, including three D. marginatus genotypes from China, was connected to these branches, forming part of the broader D. marginatus clade (Fig. S17). The D. raskemensis main clade, monophyletic to D. marginatus, is divided into two subclades with a moderate posterior probability (Posterior = 0.74). One subclade includes a reference sequence from Türkiye (D. raskemensis isolate IT-D1109, PP618825), while the other (DnmIT) comprises records from Iran, including three D. niveus and one D. marginatus (Fig. S17). A separate genogroup (DsnIT), containing four D. silvarum records from China and one D. niveus record from Iran, was externally linked to the D. marginatus and D. raskemensis clades with low posterior probability (posterior = 0.2). The phylogenetic analysis of the D. silvarum/nuttalli clade revealed a complex structure with 122 sequences organized into four genogroups and one distinct branch. The first genogroup, DnsIT1, is the largest, comprising 79 genotypes primarily identified as D. nuttalli, alongside a single D. silvarum sequence. These records were distributed across China, Mongolia, and Russia. The second genogroup, DnsIT2, included 24 D. nuttalli and four D. silvarum genotypes, also originating from China and Mongolia. The third genogroup, DnsIT3, was exclusively composed of nine D. nuttalli genotypes from Mongolia. The fourth genogroup, DnsIT4, contained six D. marginatus genotypes from China, while a separate clade consisted of a single D. nuttalli genotype (D. nuttalli isolate NM68, MW477873) from Mongolia, forming a distinct lineage (Fig. S17). Detailed information on sequences and genogroups can be found in Table

The phylogenetic analysis of genotypes characterized in this study revealed that all genotypes clustered within the *D. marginatus* main clade, specifically into the genogroup DmIT1, which is the largest group in this clade and includes *D. marginatus*, *D. niveus*, and *D. silvarum* records from European and Asian specimens (Fig. S17). Within this genogroup, the genotypes were further divided into two distinct subgroups supported by maximum posterior probability. One subgroup consisted of 11 genotypes (four from NE, three from CN, and four shared genotypes), while the second subgroup contained 93 genotypes (34 from CN, 35 from NE, and 24 shared genotypes) (Fig. S16.b). Interestingly, *D. marginatus* records in the phylogenetic tree displayed notable paraphyly. The genogroup DnsIT4, comprising six *D. marginatus* records from China, was found to be paraphyletic with the *D. marginatus* main clade. Instead, this group was monophyletic with a *D. nuttalli* genogroup (DnsIT3) supported by a high posterior probability (posterior = 0.85), clustering into the *D. silvarum/nuttalli* main clade. Furthermore, *D. niveus* records did not form a distinct and separate clade with sufficient posterior probability support. Instead, *D. niveus* sequences were found in mixed clades alongside *D. marginatus* and *D. silvarum* records (Fig. S17).

Discussion

Dermacentor marginatus is a medically significant tick species with a broad distribution across Europe, Asia, and North Africa, thriving in diverse habitats, and acting as a vector for various pathogens^{10,19,20}. Predictions based on future climate scenarios suggest a potential expansion of suitable habitats for *D. marginatus*, particularly in

Europe, with significant shifts in population densities expected in certain regions⁶⁹. Despite its importance, its ecology, genetic diversity, taxonomy, and vectorial competence remain poorly understood, leading to gaps in research on its role in human and animal health^{9,10}. Additionally, unresolved classification issues within the *D. marginatus* species complex further complicate population-level studies⁸. This study represents the first comprehensive population genetic analysis of *D. marginatus*, providing key insights into its population structure, genetic diversity, and potential evolutionary dynamics. These findings lay the groundwork for future research on this underexplored yet medically important tick species.

Population structure and demographic history of *D. marginatus* upon its Anatolian populations

Our findings revealed a high level of genetic diversity within D. marginatus populations in Anatolia, with 71 haplotypes in CN and 64 in NE, with only four shared between regions, This level of differentiation is consistent with previous reports from Romania and Kazakhstan, where intraspecific variation in cox1 ranged from 0.1% to 1% and 0.12% to 1.94%, respectively 70,71. However, unlike these studies, our dataset provides greater haplotype-level resolution, covering a broader geographic scale with a significantly larger sample size. Additional studies from Croatia, Iran, Kazakhstan, China, and Pakistan have reported cox1 sequences for a small number of specimens⁷²⁻⁷⁵, but the absence of detailed haplotype-level data prevents meaningful comparisons. Similarly, ITS2-based analyses identified 65 genotypes in CN and 67 in NE, with 28 shared between regions. While previous studies from Romania and Iran reported limited ITS2 variation (0.9% to 1.2%)^{76,77}, our findings suggest greater genetic diversity in Anatolia. The lack of detailed haplotype and genotype data in earlier studies has limited direct comparisons^{72,78–80}, but our results a valuable reference dataset for future phylogeographic studies. Overall, our study presents the first comprehensive population genetic assessment of D. marginatus. The high number of novel haplotypes and genotypes identified suggests that this species' genetic diversity was likely underestimated due to limited sampling and restricted geographic coverage. These findings emphasize the need for expanded, region-wide genetic studies to better understand the evolutionary history and population dynamics of *D. marginatus*.

The significant haplotype diversity observed in *D. marginatus* (131 haplotypes) in Anatolia notably higher than that of other *Dermacentor* species. For example, *D. reticulatus* populations in Europe generally exhibit lower genetic diversity across similar geographic regions^{6,16,18}. This may reflect differences in ecological conditions, evolutionary history, and dispersal patterns between species. The higher genetic diversity in *D. marginatus* suggests that Anatolia's diverse ecological and climatic gradients promote genetic differentiation and isolation. In contrast, a study on *Hyalomma marginatum* in Türkiye found relatively low genetic diversity despite its broad distribution across nine locations. Using microsatellite markers, the study reported moderate genetic differentiation between populations, likely due to limited gene flow influenced by anthropogenic factors such as livestock transport and environmental conditions⁸¹. The ecological diversity of Anatolia may explain the higher genetic variations in *D. marginatus* compared to these species. However, biotic factors specific to *D. marginatus* may also contribute to its genetic structure. These findings underscore the combined influence of environmental and biotic factors in shaping tick population genetics. Future studies incorporating ecological data, host interactions, and microbiota dynamics will be crucial to understanding how climatic conditions and geographic barriers influence *D. marginatus* populations in Anatolia.

This study identified a high proportion of haplotypes and genotypes at both the cox1 and ITS2 loci, with cox1 exhibiting greater variability and informativeness than ITS2. This pattern is consistent with findings in other tick species, where mitochondrial genes typically show higher diversity and utility in population genetic studies compared to nuclear markers^{12,42,82–84}. Given the scarcity of D. marginatus population genetic data, direct comparisons with other geographic regions were not possible, and population structure was analyzed within Anatolia. While analyses were conducted using cox1, ITS2, and concatenated datasets, primary inferences were based on cox1, with ITS2 and the concatenated dataset serving as complementary data. Neutrality tests based on cox1 rejected the null hypothesis of neutral evolution, suggesting recent demographic expansion within Anatolian D. marginatus populations. This was further supported by a unimodal mismatch distribution pattern and confirmed by the concatenated dataset. Under a population expansion model, haplotype diversity is expected to be high while nucleotide diversity remains low, as newly haplotypes are retained in the population^{52,53,85}. Our results align with this expectation, with high haplotype diversity (Hd=0.9283) and low nucleotide diversity (H=0.00319). Similar demographic expansion patterns have been reported in other tick species, including D. Teticulatus in Eurasia¹⁸, D. Teticulatus in Eurasia¹⁸, Teticulatus in the USA¹³, Teticulatus in Central Africa⁸⁴. The observed demographic expansion in Teticulatus populations may be driven by a combination of geographic, environmental, and anthropogenic factors.

The cox1 gene-level analyses confirmed great genetic differentiation between CN and NE populations, as indicated by AMOVA and F_{ST} values s. STRUCTURE analyses further supported this by identifying distinct genetic clusters in each region. Additionally, SAMOVA results showed that CN populations generally formed a single cluster, whereas NE populations were divided into multiple subgroups, suggesting partial geographic isolation. Gene flow between CN and NE was limited, as reflected in the small number of shared haplotypes and the estimated Nm value (2.31). Notably, gene flow was higher within CN than NE populations, possibly indicating subpopulation structuring in the latter. These patterns highlight the need for rapidly evolving markers, such as microsatellites, to achieve finer resolution of genetic structure. The Anatolian Diagonal appears to act as a potential partial barrier to gene flow, with higher genetic diversity in NE likely influenced by its greater topographical and climatic heterogeneity 31. Additionally, the eastern region of Anatolia, particularly beyond the Anatolian Diagonal, is characterized by generally higher elevations compared to the west. This topographical difference might contribute to the observed genetic differentiation, potentially influencing habitat suitability and dispersal patterns. However, confirming the direct impact of elevation and other environmental factors on

D. marginatus populations requires further ecological and landscape-level analyses in future studies. While this study primarily focused on genetic and geographic distances, ecological factors such as host availability, climatic conditions, and habitat suitability undoubtedly play crucial roles in shaping population structure, as previously shown in tick population studies^{1,5,69}.

The haplotype network and distribution analysis revealed that CN has two dominant region-specific haplotypes widely distributed across sampling sites, in addition to 16 haplotypes represented by multiple samples. In contrast, NE lacked a widely dominant region-specific haplotype, with haplotypes being more evenly distributed. These findings suggest that random mating appears more frequent in CN populations, as indicated by higher gene flow and panmictic structures. Meanwhile, gene flow in NE populations appears more restricted, with shared haplotypes being more common than unique ones. This supports the idea that NE may be the primary source of shared haplotypes, given the limited but ongoing dispersal trend from east to west across the Anatolian Diagonal. These observations indicate that the *D. marginatus* populations in CN and NE are shaped by distinct structuring and dispersal patterns. Historically, Anatolia has served as a biological refuge, fostering high biodiversity and driving species evolution⁸⁷, which likely contributed to the observed genetic diversity in *D. marginatus*.

The Anatolian Diagonal, first proposed in the 1970s³⁴, is a major biogeographical barrier shaping species differentiation in the region. It separates two distinct phytogeographical zones: Central Anatolia, with elevations typically below 1500 m, and Eastern Anatolia, generally above this threshold. The diagonal extends from northeastern Anatolia (Bayburt-Gümüşhane) southwestward to the Mediterranean Sea, splitting into two branches upon reaching the Central Taurus Mountains^{88,89}. This geographical structure has played a crucial role in biodiversity and ecological patterns, particularly by restricting dispersal and promoting endemic speciation^{27,29,30,32,90-92}. Several factors contribute to its impact on population structuring, including physical, ecological, and climatic contrasts, as well as the palaeogeological history of Anatolia^{30,34,90}. In *D. marginatus*, these geographic barriers likely shape population differentiation, with palaeogeological and environmental factors influencing genetic structuring on either side of the diagonal. In addition to abiotic factors, biotic elements, including host availability and microbiotic interactions, may also play a role in tick population structuring 93,94. However, complete genetic isolation is absent, as indicated by limited but ongoing gene flow from NE to CN, aligning with the broader ecological influence of the Anatolian Diagonal. Human-mediated factors, particularly livestock movement from Eastern to Central Anatolia, likely facilitate haplotype dispersal and influence the natural gene flow of D. marginatus. Annual large-scale animal transport between these regions could partially explain the observed genetic connectivity, despite geographic barriers.

The Anatolian Diagonal acts as a potential geographic barrier to gene flow in *D. marginatus*, yet climatic changes, habitat fragmentation, and host dynamics also shape its population structure. Climatic shifts may have facilitated *D. marginatus* expansion into new habitats, while host movement, particularly livestock migration, plays a key role in tick dispersal^{95–97}. Anthropogenic activities, such as agriculture and livestock migration, both facilitate gene flow and cause habitat fragmentation, potentially isolating populations. However, human-mediated movement often maintains connectivity, contributing to the observed demographic expansion^{95,98}. In addition to these drivers, the stepping-stone model of gene flow may explain the genetic structure of *D. marginatus*, where populations are linked through intermediate barriers, allowing limited gene flow across smaller obstacles but restricting movement in more significant barriers. A similar pattern has been observed in *Anopheles* spp., where gene flow occurs between neighboring populations⁹⁹. Furthermore, historical climatic events, such as glaciation, likely influenced population bottlenecks or expansions, contributing to genetic differentiation^{100,101}. These historical and contemporary forces, combined with ecological and geographic barriers, shape the current genetic structure of *D. marginatus* in Anatolia.

Research on several tick species, including *D. marginatus*, emphasizes the importance of integrating ecological niche modeling (ENM) and landscape analysis in understanding tick distribution and population dynamics^{20,97,102,103}. However, ENM remains underutilized in tick population genetics. Integrating ENM and landscape genetics could clarify the ecological and environmental drivers of *D. marginatus* population structure. By combining genetic data with habitat and climatic models, future studies can identify key factors influencing geographic isolation and differentiation, providing deeper insights into the evolutionary dynamics and biogeographic patterns of *D. marginatus* across Anatolia and beyond.

This study provides key insights into the population genetics of *D. marginatus* in Anatolia. However, comparisons with other regions are needed to contextualize these findings. Currently, no population genetic data exist for *D. marginatus* to allow direct comparisons, but similar genetic structuring patterns have been reported in other *Dermacentor* species. For example, studies on *D. variabilis* (American dog tick) revealed genetic differentiation driven by ecological barriers and host distribution 13,14,94. Comparable patterns have been observed in *D. andersoni* and *D. albipictus* in the New World4,12,15,104,105, and in *D. reticulatus* in the Old World6,7,18. These findings support the role of ecological and geographic factors in shaping tick population structure, as observed in *D. marginatus*. Future studies should expand analyses to other regions within the species' distribution, incorporating a broader geographic range to explore cryptic genetic relationships.

In this study, we selected the mitochondrial *cox1* and nuclear ITS2 markers due to their widespread use in tick population genetics and ability to detect genetic differentiation across large geographic scales^{1,42,84,106,107}. While reliable for genetic studies, these markers are relatively conserved and provide lower resolution than microsatellites or SNPs¹. The lack of a reference genome and microsatellite library for *D. marginatus* limited the application of such approaches. Despite this, *cox1* revealed strong genetic structuring, highlighting the need for future studies using more variable markers. This study provides the first detailed population genetic analysis of *D. marginatus*, laying the groundwork for further research. While our findings offer valuable insights, incorporating genome-wide markers, such as SNPs, could refine our understanding of genetic differentiation and gene flow. Future research should focus on integrating higher-resolution markers and next-generation

sequencing technologies to uncover fine-scale genetic patterns. Additionally, predictive models assessing *D. marginatus* distribution under future climatic conditions could help anticipate climate change impacts and improve management strategies. Comparing *D. marginatus* with other tick species would also clarify whether the Anatolian Diagonal influences their genetic structure similarly. These efforts will enhance our understanding of the ecological and evolutionary processes shaping tick populations across Anatolia and beyond.

Phylogenetic structure of Dermacentor marginatus

Bayesian inference was used to assess the phylogenetic relationships of haplotypes/genotypes, their placement within the D. marginatus complex, and the structure of the subgenus Serdjukovia. Despite significant cladistic divergence, populations did not form distinct region-specific clades in phylogenetic trees. This likely reflects incomplete isolation and the presence of shared haplotypes between CN and NE populations. Notably, haplotype CX-NE54 was highly divergent in the cox1 phylogeny, clustering separately from other haplotypes. Found at sampling site L24 in NE, CX-NE54 exhibited the highest pairwise divergence among cox1 haplotypes. The cox1 tree for Serdjukovia showed that the 130 haplotypes in this study formed a well-supported large clade, divided into two subclades: Dm1a, predominantly from NE, and Dm1b, mainly from CN. Both subclades clustered with specimens from Europe, Asia, and North Africa. Interestingly, CX-NE54 grouped within a distinct Central Asian haplogroup (Dm2) along with specimens from the Xinjiang Uygur Autonomous Region (China) and Kazakhstan. This clade is monophyletic with a sister group containing specimens from China, Kazakhstan, and Russia. Morphologically, CX-NE54 shares typical characteristics of D. marginatus and shows no notable variation compared to other specimens in this clade^{71,73,82,102,108}. The presence of this highly divergent haplotype in NE suggests historical colonization events from Central Asia, potentially driven by past climatic or ecological changes. Alternatively, host movement, environmental shifts, or local ecological factors may facilitate ongoing migration. These findings underscore the complex evolutionary history of D. marginatus and the need for further research on migration and gene flow patterns. Future studies should incorporate specimens from adjacent regions to better understand dispersal dynamics and population density.

Dermacentor marginatus phylogeny within the subgenus Serdjukovia revealed five haplogroups and three distinct branches. Previous studies on D. marginatus phylogeny were based on limited specimen numbers, providing only partial insights 11,72,73,75,79,80,108-110. This study presents, for the first time, a detailed phylogenetic structure of D. marginatus at the clade, haplogroup, and branch levels. The cox1-based phylogenetic tree showed that D. niveus records from China clustered with D. marginatus from China and Kazakhstan, placing them within the main D. marginatus clade. A D. niveus record from Iran clustered within the D. raskemensis clade, forming a monophyletic group with reference specimens. Similar phylogenetic patterns were observed in the ITS2 tree. The taxonomic status of *D. niveus* remains controversial, with some authors considering it a synonym of D. marginatus, while others argue for its recognition as a separate species until proven otherwise^{8,38,39,78}. The phylogenetic trees in this study did not support clear separation between D. niveus and D. marginatus. However, potential misidentifications in existing D. niveus records or the absence of morpho-molecular data from confirmed specimens prevent definitive conclusions. As suggested by Guglielmone et al. (2020)8, a thorough characterization of the type specimen (or holotype, neotype) is necessary. No Anatolian specimens in this study matched the D. niveus morphotype, despite past reports from both study regions 21,22,35,36,111,112 . This suggests that earlier reports may require reevaluation, and D. marginatus phenotypic variants could have been misidentified as D. niveus, particularly in Anatolia. A definitive conclusion will require a reassessment of previously reported D. niveus specimens, if available. Overall, these results strongly indicate that regardless of whether D. niveus is validated as a separate species, D. marginatus is a cryptic tick species with substantial phenotypic and genotypic diversity.

This study also provided key phylogenetic insights into other *Serdjukovia* species. Notably, *D. raskemensis*, first genetically characterized only recently¹¹³, emerged as a key species of interest. A specimen previously listed in GenBank as *D. niveus* from Iran—entered before the first *D. raskemensis* reference sequence became available⁷²—clustered within the *D. raskemensis* main clade in the *cox1* phylogeny. This suggests that the Iranian specimen may actually be *D. raskemensis*. Morphological records of *D. raskemensis* from Iran have been documented in the past¹¹⁴, further supporting this reclassification. Additionally, this study provided the first ITS2 sequence for a *D. raskemensis* reference specimen, establishing a crucial genetic record for future research. Our findings, along with previous results¹¹³, strongly indicate that *D. marginatus* and *D. raskemensis* share a sister phylogenetic relationship. This close relationship raises the possibility of sympatric speciation between these two species.

The phylogenetic trees from both genes also provided insights into the relationship between *D. nuttalli* and *D. silvarum* within *Serdjukovia*. Based on GenBank records, these species could not be clearly distinguished at the *cox1* and ITS2 levels. The *cox1* phylogeny showed that the *D. nuttalli/silvarum* main clade was distinct from other *Serdjukovia* species, a pattern also confirmed in the ITS2 phylogeny. However, within this main clade, they formed mixed haplogroups in the *cox1* tree, lacking clear differentiation. This ambiguity may result from misidentifications in GenBank or taxonomic uncertainty, similar to *D. marginatus* and *D. niveus*. The ITS2 phylogeny further highlighted this complexity, as a genogroup (DnsIT4) containing *D. marginatus* records from China clustered within the *D. nuttalli/silvarum* main clade, alongside erroneous GenBank records. These findings underscore significant database errors, particularly regarding *D. nuttalli/silvarum* records. To resolve these taxonomic uncertainties, clear morphological and genetic definitions are needed, particularly for Chinese samples. A standardized approach is necessary to correct these discrepancies and refine the phylogenetic framework for these species.

Conclusion

This study provides the most comprehensive population genetic and phylogenetic analysis of *D. marginatus* to date. *Dermacentor marginatus* in Anatolia exhibited remarkable genetic diversity, with all 131 haplotypes being unique. The findings suggest a recent demographic expansion, likely shaped by ecological and biogeographical factors. The Anatolian Diagonal acts as a potential biogeographical barrier, shaping *D. marginatus* genetic structure. While population structuring indicates geographic isolation between CN and NE, some gene flow persists between these regions. Gene flow was higher within CN than NE, reflecting regional ecological and geographic differences.

These results underscore the Anatolian Diagonal's potential role in shaping *D. marginatus* populations within this biodiversity hotspot and its broader influence on the region's biogeography. The presence of a divergent *D. marginatus* haplotype clustering with Central Asian samples suggests historical dispersal and evolutionary links. Phylogenetic analyses also revealed unresolved taxonomic issues within subgenus *Serdjukovia*, particularly regarding *D. niveus*, which may not form a distinct clade. Additionally, misidentified records of *D. marginatus* and *D. raskemensis*, as well as taxonomic ambiguities between *D. nuttalli* and *D. silvarum*, were highlighted. Furthermore, the monophyletic relationship between *D. marginatus* and *D. raskemensis* supports the hypothesis of sympatric speciation, highlighting the region's evolutionary complexity. This study advances our understanding of *D. marginatus* population genetics and phylogeography, laying the foundation for future research on the ecological and biogeographical dynamics of parasites and their hosts in Anatolia.

Data availability

The sequence data that support the findings of this study are openly available in GenBank (https://www.ncbi.n lm.nih.gov/genbank/) and BOLD (http://www.boldsystems.org) databases under accession numbers/barcodes provided in Table S8 and Table S15. The geographical coordinates of locations are provided in Table S1 and BOLD database. All data involved in this study are available from the corresponding author upon request. Correspondence and data requests should be addressed to Ö.O (omerorkun@yahoo.com.tr).

Received: 9 July 2024; Accepted: 7 April 2025

Published online: 12 April 2025

References

- Araya-Anchetta, A., Busch, J. D., Scoles, G. A. & Wagner, D. M. Thirty years of tick population genetics: A comprehensive review. Infect. Genet. Evol. 29, 164–179 (2015).
- 2. Kozakiewicz, C. P. et al. Pathogens in space: Advancing understanding of pathogen dynamics and disease ecology through landscape genetics. *Evol. Appl.* 11, 1763–1778 (2018).
- 3. Lado, P. et al. Integrating population genetic structure, microbiome, and pathogens presence data in Dermacentor variabilis. *PeerJ* 7, e9367 (2020).
- 4. De La Fuente, J. et al. Characterization of genetic diversity in *Dermacentor andersoni* (Acari: Ixodidae) with body size and weight polymorphism. *Exp. Parasitol.* **109**, 16–26 (2005).
- 5. Beati, L. & Klompen, H. Phylogeography of ticks (Acari: Ixodida). Annu. Rev. Entomol. 64, 379-397 (2019).
- Kloch, A. et al. Origins of recently emerged foci of the tick Dermacentor reticulatus in central Europe inferred from molecular markers. Vet. Parasitol. 237, 63–69 (2017).
- Paulauskas, A. et al. Microsatellite-based genetic diversity of Dermacentor reticulatus in Europe. Infect. Genet. Evol. 66, 200–209 (2018).
- 8. Guglielmone, A. A., Petney, T. N. & Robbins, R. G. Ixodidae (Acari: Ixodea): Descriptions and redescriptions of all known species from 1758 to December 31, 2019. *Zootaxa* **4871**, 1–322 (2020).
- 9. Guglielmone, A. A., Nava, S. & Robbins, R. G. Geographic distribution of the hard ticks (Acari: Ixodida: Ixodidae) of the world by countries and territories. *Zootaxa* **5251**, 1–274 (2023).
- Hornok, S. Dermacentor marginatus (Sulzer, 1776) (Figs. 111–113). In Ticks of Europe and North Africa 281–285 (Springer, Cham, 2017). https://doi.org/10.1007/978-3-319-63760-0_54.
- 11. Wang, F. et al. Species delimitation of the *Dermacentor* ticks based on phylogenetic clustering and niche modeling. *PeerJ* 2019, e6911 (2019).
- Leo, S. S. T., Pybus, M. J. & Sperling, F. A. H. Deep mitochondrial DNA lineage divergences within Alberta populations of Dermacentor albipictus (Acari: Ixodidae): Do not indicate distinct species. J. Med. Entomol. 47, 565–574 (2010).
- 13. Krakowetz, C. N., Dergousoff, S. J. & Chilton, N. B. Genetic variation in the mitochondrial 16S rRNA gene of the American dog tick, *Dermacentor variabilis* (Acari: Ixodidae). *J. Vector Ecol.* 35, 163–173 (2010).
- 14. Lado, P., Cox, C., Wideman, K., Hernandez, A. & Klompen, H. Population genetics of *Dermacentor variabilis* Say 1821 (Ixodida: Ixodidae) in the United States inferred from ddRAD-seq SNP markers. *Ann. Entomol. Soc. Am.* 112, 433–442 (2019).
- Reynolds, S., Hedberg, M., Herrin, B. & Chelladurai, J. R. J. J. Analysis of the complete mitochondrial genomes of *Dermacentor albipictus* suggests a species complex. *Ticks Tick Borne Dis.* 13, 102038 (2022).
- Movila, A., Morozov, A. & Sitnicova, N. Genetic polymorphism of 12S rRNA gene among *Dermacentor reticulatus* Fabricius ticks in the Chernobyl Nuclear Power Plant Exclusion Zone. *J. Parasitol.* 99, 40–43 (2013).
- 17. Olivieri, E. et al. The southernmost foci of *Dermacentor reticulatus* in Italy and associated *Babesia canis* infection in dogs. *Parasit. Vectors* 9, 1–9 (2016).
- 18. Bilbija, B. et al. *Dermacentor reticulatus* a tick on its way from glacial refugia to a panmictic Eurasian population. *Int. J. Parasitol.* 53, 91–101 (2023).
- 19. Rubel, F. et al. Geographical distribution of *Dermacentor marginatus* and *Dermacentor reticulatus* in Europe. *Ticks Tick Borne Dis.* 7, 224–233 (2016).
- Walter, M., Brugger, K. & Rubel, F. The ecological niche of Dermacentor marginatus in Germany. Parasitol. Res 115, 2165–2174 (2016).
- 21 Kurtpınar, H. Türkiye Keneleri (Morfoloji, Biyoloji, Konakçı, Yayılışları ve Medikal Önemleri) (Güven matbaası, 1954).
- 22. Merdivenci, A. *Türkiye Keneleri Üzerine Araştırmalar* (İstanbul Üniversitesi Cerrahpaşa Tıp Fakültesi Yayınları, 1969).
- 23. Orkun, Ö. Some Ecological and Epidemiological Data Belonging to tick Species in Ankara and Around (Ankara University, 2015).
- 24. Nosek, J. The ecology and public health importance of *Dermacentor marginatus* and *D. reticulatus* ticks in Central Europe. *Folia Parasitol (Praha)* 19, 93–102 (1972).

- Parola, P. et al. Update on tick-borne rickettsioses around the world: A geographic approach. Clin. Microbiol. Rev. 26, 657–702 (2013).
- 26. Filippova, N. A. Fauna of Russia and Neighboring Countries, Arachnoidea, Colume IV, Issue 5, Ixodid Ticks of Subfamily Amblyomminae (Nauka Publishing House, 1997).
- Bilgin, R. Back to the Suture: The distribution of intraspecific genetic diversity in and around Anatolia. Int. J. Mol. Sci. 12, 4080–4103 (2011).
- 28. Uslu, E., Bakiş, Y. & Babaç, M. A study on biogeographical distribution of Turkish oak species and their relations with the Anatolian Diagonal. *Acta Bot. Hung.* 53, 423–440 (2011).
- 29. Gül, S. Ecological divergence between two evolutionary lineages of *Hyla savignyi* (Audouin, 1827) in Turkey: Effects of the Anatolian Diagonal. *Anim. Biol.* **63**, 285–295 (2013).
- 30. Gür, H. The Anatolian diagonal revisited: Testing the ecological basis of a biogeographic boundary. *Zool. Middle East* **62**, 189–199 (2016).
- 31. Gür, H. Anadolu Diyagonali: Bir biyocoğrafi sınırın anatomisi. Kebikeç İnsan Bilimleri İçin Kaynak Araştırmaları Dergisi 0, 177–188 (2017).
- 32. Korkmaz, E. M., Lunt, D. H., Çiplak, B., Değerli, N. & Başibüyük, H. H. The contribution of Anatolia to European phylogeography: The centre of origin of the meadow grasshopper, *Chorthippus parallelus*. *J. Biogeogr.* 41, 1793–1805 (2014).
- 33. Mutun, S. & Dinç, S. The Anatolian diagonal and paleoclimatic changes shaped the phylogeography of *Cynips quercus* (Hymenoptera, Cynipidae). *Ann. Zool. Fennici* **56**, 65–83 (2019).
- Davis, P. H. Distribution patterns in Anatolia with particular reference to endemism. In *Plant Life of South-West Asia* (eds Davis, P. H. et al.) 15–27 (The Botanical Society of Edinburgh, 1971).
- 35. Özkan, M. Erzurum ve çevre illeri kenelerinin sistematik yönden incelenmesi (Atatürk Üniversitesi, 1976).
- 36. Arslan, M. Ö., Umur, Ş & Aydın, L. Kars yöresi sığırlarında Ixodidae türlerinin yaygınlığı. *Türkiye Parazitoloji Dergisi* 23, 331–335 (1999).
- 37. Pomerantzev, B. I. Ixodid Ticks (Ixodidae). In Fauna of the USSR, New Series 41: Arachnoidea (Leningrad, 1950).
- 38. Arthur, D. R. Ticks. A Monograph of the Ixodea. Part V. On the Genera Dermacentor, Anocentor, Cosmiomma, Boophilus and Margaropus (Cambridge University Press, 1960).
- 39 Estrada-Peña, A. & Estrada-Peña, R. Notes on Dermacentor ticks: Redescription of *D. marginatus* with the synonymies of *D. niveus* and *D. daghestanicus* (Acari: Ixodidae). *J. Med. Entomol.* 28, 1–15 (1991).
- Filipova, N. A. & Palaksina, M. A. Some aspects of intraspecific variability of the closely related species of the *Dermacentor marginatus* complex (Acari: Ixodidae) as demonstration of microevolutionary process. *Parazitologiia* 39, 337–364 (2005).
- 41. Barker, S. C. Distinguishing species and populations of rhipicephaline ticks with its 2 ribosomal RNA. *J. Parasitol.* **84**, 887–892 (1998).
- 42. Song, S., Shao, R., Atwell, R., Barker, S. & Vankan, D. Phylogenetic and phylogeographic relationships in *Ixodes holocyclus* and *Ixodes cornuatus* (Acari: Ixodidae) inferred from COX1 and ITS2 sequences. *Int. J. Parasitol.* 41, 871–880 (2011).
- 43. Larsson, A. AliView: A fast and lightweight alignment viewer and editor for large datasets. *Bioinformatics* **30**, 3276–3278 (2014).
- 44. Katoh, K., Rozewicki, J. & Yamada, K. D. MAFFT online service: Multiple sequence alignment, interactive sequence choice and visualization. *Brief Bioinform.* 20, 1160–1166 (2019).
- 45. Rozas, J. et al. DnaSP 6: DNA Sequence polymorphism analysis of large data sets. Mol. Biol. Evol. 34, 3299-3302 (2017).
- 46. Rogers, A. R. & Harpending, H. Population growth makes waves in the distribution of pairwise genetic differences. *Mol. Biol. Evol.* **9**, 552–569 (1992).
- 47. Clement, M., Posada, D. & Crandall, K. A. TCS: A computer program to estimate gene genealogies. *Mol. Ecol.* **9**, 1657–1659 (2000).
- 48 Múrias Dos Santos, A., Cabezas, M. P., Tavares, A. I., Xavier, R. & Branco, M. tcsBU: A tool to extend TCS network layout and visualization. *Bioinformatics* 32, 627–628 (2016).
- 49. Tamura, K., Stecher, G. & Kumar, S. MEGA11: Molecular evolutionary genetics analysis version 11. Mol. Biol. Evol. 38, 3022–3027 (2021).
- 50. Muhire, B. M., Varsani, A. & Martin, D. P. SDT: A virus classification tool based on pairwise sequence alignment and identity calculation. *PLoS ONE* 9, e108277 (2014).
- 51. Tajima, F. Statistical method for testing the neutral mutation hypothesis by DNA polymorphism. Genetics 123, 585 (1989).
- 52. Fu, Y. X. Statistical tests of neutrality of mutations against population growth, hitchhiking and background selection. *Genetics* 147, 915–925 (1997).
- 53 Excoffier, L. & Lischer, H. E. L. Arlequin suite ver 3.5: A new series of programs to perform population genetics analyses under Linux and Windows. *Mol. Ecol. Resour.* 10, 564–567 (2010).
- Excoffier, L., Smouse, P. E. & Quattro, J. M. Analysis of molecular variance inferred from metric distances among DNA haplotypes: Application to human mitochondrial DNA restriction data. *Genetics* 131, 479–491 (1992).
- Wright, S. The interpretation of population structure by f-statistics with special regard to systems of mating. Evolution 19, 395–420 (1965).
- 56. Pritchard, J. K., Stephens, M. & Donnelly, P. Inference of population structure using multilocus genotype data. *Genetics* 155, 945–959 (2000).
- 57. Falush, D., Stephens, M. & Pritchard, J. K. Inference of population structure using multilocus genotype data: Linked loci and correlated allele frequencies. *Genetics* 164, 1567–1587 (2003).
- 58. Francis, R. M. pophelper: An R package and web app to analyse and visualize population structure. *Mol. Ecol. Resour.* 17, 27–32 (2017)
- 59. Mantel, N. The detection of disease clustering and a generalized regression approach. *Cancer Res.* **27**, 209–220 (1967).
- Dupanloup, I., Schneider, S. & Excoffier, L. A simulated annealing approach to define the genetic structure of populations. Mol. Ecol. 11, 2571–2581 (2002).
- 61 Paradis, E. & Schliep, K. ape 5.0: An environment for modern phylogenetics and evolutionary analyses in R. *Bioinformatics* **35**, 526–528 (2019).
- Padgham, M. Geodist: Fast, dependency-free geodesic distance calculations. R package version 0.0.7. https://github.com/hypertidy/geodist. (2021) https://doi.org/10.1007/s00190-012-0578-z.
- 63. Sela, I., Ashkenazy, H., Katoh, K. & Pupko, T. GUIDANCE2: Accurate detection of unreliable alignment regions accounting for the uncertainty of multiple parameters. *Nucleic Acids Res.* 43, W7–W14 (2015).
- 64. Edgar, R. C. MUSCLE: A multiple sequence alignment method with reduced time and space complexity. *BMC Bioinform.* 5, 113 (2004).
- 65. Darriba, D., Taboada, G. L., Doallo, R. & Posada, D. jModelTest 2: More models, new heuristics and parallel computing. *Nat. Methods* 9, 772–772 (2012).
 66. Darriba, D. et al. ModelTest-NG: A new and scalable tool for the selection of DNA and protein evolutionary models. *Mol. Biol.*
- Evol. 37, 291–294 (2020).

 67 Bouckaert, R. et al. BEAST 2.5: An advanced software platform for Bayesian evolutionary analysis. PLoS Comput. Biol. 15,
- 67 Bouckaert, R. et al. BEAST 2.5: An advanced software platform for Bayesian evolutionary analysis. *PLoS Comput. Biol.* 15, e1006650 (2019).
- 68 Rambaut, A., Drummond, A. J., Xie, D., Baele, G. & Suchard, M. A. Posterior summarization in Bayesian phylogenetics using Tracer 1.7. Syst. Biol. 67, 901–904 (2018).

- 69. Cunze, S., Glock, G., Kochmann, J. & Klimpel, S. Ticks on the move—climate change-induced range shifts of three tick species in Europe: Current and future habitat suitability for *Ixodes ricinus* in comparison with *Dermacentor reticulatus* and *Dermacentor marginatus*. *Parasitol. Res.* 121, 2241–2252 (2022).
- 70. Chitimia, L. et al. Genetic characterization of ticks from southwestern Romania by sequences of mitochondrial cox1 and nad5 genes. Exp. Appl. Acarol. 52, 305–311 (2010).
- 71. Zheng, Z. et al. Application of DNA barcodes in the genetic diversity of hard ticks (Acari: Ixodidae) in Kazakhstan. Exp. Appl. Acarol. 92, 547–554 (2024).
- 72. Soltan-Alinejad, P. et al. Molecular characterization of Ribosomal DNA (ITS2) of hard ticks in Iran: Understanding the conspecificity of *Dermacentor marginatus* and *D. niveus. BMC Res. Notes* 13, 1–6 (2020).
- 73. Yang, Y. et al. Genetic Diversity of Hard Ticks (Acari: Ixodidae) in the South and East Regions of Kazakhstan and Northwestern China. Korean J. Parasitol. 59, 103–108 (2021).
- 74. Krčmar, S. et al. DNA barcoding of hard ticks (Ixodidae), notes on distribution of vector species and new faunal record for Croatia. *Ticks Tick Borne Dis.* 13, 101920 (2022).
- 75. Ahmad, I. et al. First molecular-based confirmation of *Dermacentor marginatus* and associated *Rickettsia raoultii* and *Anaplasma marginale* in the Hindu Kush Mountain Range. *Animals* 13, 3686 (2023).
- 76. Chitimia, L. et al. Molecular characterization of hard and soft ticks from Romania by sequences of the internal transcribed spacers of ribosomal DNA. *Parasitol. Res.* **105**, 907–911 (2009).
- 77. Abdigoudarzi, M., Noureddine, R., Seitzer, U. & Ahmed, J. rDNA-ITS2 Identification of Hyalomma, Rhipicephalus, Dermacentor and *Boophilus* spp. (Acari: Ixodidae) collected from different geographical regions of Iran. *Adv. Stud. Biol.* 3, 221–238 (2011).
- Moshaverinia, A., Shayan, P., Nabian, S. & Rahbari, S. Genetic evidence for conspecificity between *Dermacentor marginatus* and *Dermacentor niveus*. *Parasitol. Res.* 105, 1125–1132 (2009).
- 79. Nadim, A., Khanjani, M., Hosseini-Chegeni, A. & Telmadarraiy, Z. Identity and microbial agents related to *Dermacentor marginatus* Sulzer (Acari: Ixodidae) with a new record of *Rickettsia slovaca* (Rickettsiales: Rickettsiaceae) in Iran. *Syst. Appl. Acarol.* 26, 367–378 (2021).
- 80. Lu, Y. et al. Exploration of multi-gene DNA Barcode markers to reveal the broad genetic diversity of field ticks (Acari: Ixodidae) in a tropical environment of Hainan Island, China. Cytogenet Genome Res. 163, 59–73 (2023).
- 81 Hekimoglu, O., Kuyucu, A. C. & Ozer, N. Preliminary investigation on the genetic diversity and population structure of *Hyalomma marginatum* (Acari: Ixodidae) in Turkey. *Syst. Appl. Acarol.* **25**, 1867–1882 (2020).
- 82. Lv, J. et al. Assessment of four DNA fragments (COI, 16S rDNA, ITS2, 12S rDNA) for species identification of the Ixodida (Acari: Ixodida). Parasit. Vectors 7, 1–11 (2014).
- 83. Zhang, R. L. & Zhang, B. Prospects of using DNA barcoding for species identification and evaluation of the accuracy of sequence databases for ticks (Acari: Ixodida). *Ticks Tick Borne Dis.* 5, 352–358 (2014).
- 84. Amzati, G. S. et al. Mitochondrial phylogeography and population structure of the cattle tick *Rhipicephalus appendiculatus* in the African Great Lakes region. *Parasit Vectors* 11, 1–19 (2018).
- 85. Hahn, M. Molecular Population Genetics (Oxford University Press, 2018).
- 86. Kingʻori, E. M. et al. Population genetic structure of the elephant tick *Amblyomma tholloni* from different elephant populations in Kenya. *Ticks Tick Borne Dis.* 13, 101935 (2022).
- 87. Şekercioğlu, Ç. H. et al. Turkey's globally important biodiversity in crisis. Biol. Conserv. 144, 2752-2769 (2011).
- 88. Gür, H. Geç kuvaterner buzul buzullararası döngülerinin Anadolu'nun biyolojik çeşitliliği üzerine etkileri. *Türkiye Jeoloji Bülteni* **60**, 507–528 (2017).
- 89. Kuzucuoğlu, C., Çiner, A. & Kazancı, N. The geomorphological regions of Turkey. In World Geomorphological Landscapes 41–178 (Springer, Cham, 2019). https://doi.org/10.1007/978-3-030-03515-0_4.
- 90. Ekim, T. & Güner, A. The Anatolian Diagonal: Fact or fiction?. Proc. R. Soc. Edinb. Sect. B: Biol. Sci. 89, 69-77 (1986).
- 91. Çiplak, B., Demirsoy, A. & Bozcuk, A. N. Distribution of Orthoptera in relation to the Anatolian Diagonal in Turkey. *Articulata* 8, 1–20 (1993).
- 92. Vamberger, M. et al. Conservation genetics and phylogeography of the poorly known Middle Eastern terrapin *Mauremys caspica* (Testudines: Geoemydidae). *Org. Divers. Evol.* 13, 77–85 (2013).
- 93. Sassera, D. et al. 'Candidatus Midichloria mitochondrii', an endosymbiont of the tick Ixodes ricinus with a unique intramitochondrial lifestyle. Int. J. Syst. Evol. Microbiol. 56, 2535–2540 (2006).
- 94. Kaufman, E. L. et al. Range-wide genetic analysis of *Dermacentor variabilis* and its *Francisella*-like endosymbionts demonstrates phylogeographic concordance between both taxa. *Parasit. Vectors* 11, 1–11 (2018).
- 95. Keesing, F. et al. Impacts of biodiversity on the emergence and transmission of infectious diseases. *Nature* **468**, 647–652 (2010).
- 96. Ogden, N. H. & Lindsay, L. R. Effects of climate and climate change on vectors and vector-borne diseases: Ticks are different. Trends Parasitol. 32, 646–656 (2016).
- 97 Zhang, L. et al. Projecting the potential distribution areas of *Ixodes scapularis* (Acari: Ixodidae) driven by climate change. *Biology* 11, 107 (2022).
- Salkeld, D., Hopkins, S. & Hayman, D. Land use change and emerging infectious diseases. Emerging Zoonotic and Wildlife Pathogens 221–248 (2023) https://doi.org/10.1093/OSO/9780198825920.003.0011.
- Maliti, D. et al. Islands and Stepping-Stones: Comparative population structure of Anopheles gambiae sensu stricto and Anopheles arabiensis in Tanzania and implications for the spread of insecticide resistance. PLoS ONE 9, e110910 (2014).
- 100. Hewitt, G. The genetic legacy of the Quaternary ice ages. Nature 405, 907-913 (2000).
- 101. Schmitt, T. Molecular biogeography of Europe: Pleistocene cycles and postglacial trends. Front. Zool. 4, 1-13 (2007).
- Huercha, et al. MaxEnt Modeling of Dermacentor marginatus (Acari: Ixodidae) Distribution in Xinjiang, China. J. Med. Entomol. 57, 1659–1667 (2020).
- 103. Slatculescu, A. M. et al. Species distribution models for the eastern blacklegged tick, *Ixodes scapularis*, and the Lyme disease pathogen, *Borrelia burgdorferi*, in Ontario, Canada. *PLoS ONE* 15, e0238126 (2020).
- 104. Patterson, E. I., Dergousoff, S. J. & Chilton, N. B. Genetic variation in the 16S mitochondrial DNA gene of two Canadian populations of *Dermacentor andersoni* (Acari: Ixodidae). J. Med. Entomol. 46, 475–481 (2009).
- 105. Leo, S. S. T., Samuel, W. M., Pybus, M. J. & Sperling, F. A. H. Origin of *Dermacentor albipictus* (Acari: Ixodidae) on elk in the yukon, canada. J. Wildl. Dis. 50, 544–551 (2014).
- 106. Lv, J. et al. Development of a DNA barcoding system for the Ixodida (Acari: Ixodida). Mitochondrial DNA 25, 142-149 (2014).
- 107. Kanduma, E. G. et al. Analyses of mitochondrial genes reveal two sympatric but genetically divergent lineages of *Rhipicephalus appendiculatus* in Kenya. *Parasit. Vectors* **9**, 1–15 (2016).
- 108. Sang, C. et al. Tick distribution and detection of Babesia and Theileria species in Eastern and Southern Kazakhstan. Ticks Tick Borne Dis. 12, 101817 (2021).
- 109. Bogdanov, A. S., Makenov, M. T., Medyanikova, L. V., Shchouchinova, L. D. & Yakimenko, V. V. Variability of mitochondrial cytochrome oxidase first subunit gene (COI) fragments in several tick species of the marginatus group (Ixodidae, Amblyomminae, *Dermacentor*). *Biol. Bull.* **44**, 379–383 (2017).
- 110. Hekimoglu, O., Sahin, M. K., Ergan, G. & Ozer, N. A molecular phylogenetic investigation of tick species in Eastern and Southeastern Anatolia. *Ticks Tick Borne Dis.* 12, 101777 (2021).
- 111. Sayin, F. et al. Status of the tick-borne diseases in sheep and goats in Turkey. Parassitologia 39, 153-156 (1997).

| https://doi.org/10.1038/s41598-025-97658-0

- 112. Ica, A., Inci, A., Vatansever, Z. & Karaer, Z. Status of tick infestation of cattle in the Kayseri region of Turkey. *Parasitol. Res.* **101**, 167–169 (2007).
- 113. Orkun, Ö. & Vatansever, Z. Rediscovery and first genetic description of some poorly known tick species: *Haemaphysalis kopetdaghica* Kerbabaev, 1962 and *Dermacentor raskemensis* Pomerantzev, 1946. *Ticks Tick Borne Dis.* **12**, 101726 (2021).
- 114. Hoogstraal, H. & Valdez, R. Ticks (Ixodoidea) from wild sheep and goats in Iran and medical and veterinary implications. *Fieldiana Zool.* **6**, 16 (1980).

Acknowledgements

This study was carried out within the framework of the COST Action CA21170 "Prevention, anticipation and mitigation of tick-borne disease risk applying the DAMA protocol (PRAGMATICK). A certain part (only *cox1* data of 80 *D. marginatus* individuals in Central Anatolia) of the findings presented in this study are based on the MSc thesis of Anil Yılmaz supervised by Ömer Orkun at the Department of Parasitology, Graduate School of Health Sciences, Ankara University, Ankara, Türkiye.

Author contributions

Ö.O., Z.V., conceived and conceptualized the study and supervised overall investigations. Ö.O., Z.V., E.S., A.Y., M. Y., collected samples. Ö.O., Z.V., created methodology. Ö.O., E.S., A.Y., carried out laboratory analyses. Ö.O., Z.V., analyzed data and interpreted obtained results. Ö.O., wrote the manuscript. Z.V., edited the manuscript. All authors have read and agreed to the published version of the manuscript.

Funding

This study was funded by the Scientific and Technological Research Council of Türkiye (TUBITAK) ARDEB 1001 Grant No.: 121O615. The funders had no role in the study design, data collection and analysis, decision to publish, or the preparation of the manuscript.

Declarations

Competing interests

The authors declare no competing interests.

Additional information

Supplementary Information The online version contains supplementary material available at https://doi.org/10.1038/s41598-025-97658-0.

Correspondence and requests for materials should be addressed to Ö.O.

Reprints and permissions information is available at www.nature.com/reprints.

Publisher's note Springer Nature remains neutral with regard to jurisdictional claims in published maps and institutional affiliations.

Open Access This article is licensed under a Creative Commons Attribution-NonCommercial-NoDerivatives 4.0 International License, which permits any non-commercial use, sharing, distribution and reproduction in any medium or format, as long as you give appropriate credit to the original author(s) and the source, provide a link to the Creative Commons licence, and indicate if you modified the licensed material. You do not have permission under this licence to share adapted material derived from this article or parts of it. The images or other third party material in this article are included in the article's Creative Commons licence, unless indicated otherwise in a credit line to the material. If material is not included in the article's Creative Commons licence and your intended use is not permitted by statutory regulation or exceeds the permitted use, you will need to obtain permission directly from the copyright holder. To view a copy of this licence, visit http://creativecommons.org/licenses/by-nc-nd/4.0/.

© The Author(s) 2025